CONTENTS

ACHIEVING HIGHER ACCURACY IN THE GAMMA-RAY SPECTROSCOPIC ASSAY OF HOLDUP

by

P. A. Russo, T. R. Wenz, S. E. Smith, and J. F. Harris

ABSTRACT

Gamma-ray spectroscopy is an important technique for the measurement of quantities of nuclear material holdup in processing equipment. Because the equipment in large facilities dedicated to uranium isotopic enrichment, uranium/ plutonium scrap recovery or various stages of fuel fabrication is extensive, the total holdup may be large by its distribution alone, even if deposit thicknesses are small. Good accountability practices require unbiased measurements with uncertainties that are as small as possible. This paper describes new procedures for use with traditional holdup analysis methods based on gamma-ray spectroscopy. The procedures address the two sources of bias inherent in traditional gamma-ray measurements of holdup.

Holdup measurements are performed with collimated, shielded gamma-ray detectors. The measurement distance is chosen to simplify the deposit geometry to that of a point, line or area. The quantitative holdup result is based on the net count rate of a representative gamma ray. This rate is corrected for contributions from room background and for attenuation by the process equipment. Traditional holdup measurements assume that the width of the point or line deposit is very small compared to the measurement distance, and that the self-attenuation effects can be neglected. Because each point or line deposit has a finite width and because self-attenuation affects all measurements, bias is incurred in both assumptions. In both cases the bias is negative, explaining the systematically low results of gamma-ray holdup measurements.

The new procedures correct for bias that arises from both the finite-source effects and gamma-ray self-attenuation. The procedures used to correct for both of these effects apply to the generalized geometries. One common empirical parameter is used for both corrections. It self-consistently limits the total error incurred (from uncertain knowledge of this parameter) in the combined correction process, so that it is compelling to use these procedures. The algorithms and the procedures are simple, general, and easily automated for use plant-wide.

This paper shows the derivation of the new, generalized correction algorithms for finite-source and self-attenuation effects. It also presents an analysis of the sensitivity of the holdup result to the uncertainty in the empirical parameter when one or both corrections are made. The paper uses specific examples of the magnitudes of finite-source and self-attenuation corrections to measurements that were made in the field. It discusses the automated implementation of the correction procedure.

I. INTRODUCTION

Gamma-ray spectroscopy is an important technique for the measurement of quantities of nuclear material holdup in processing equipment. Because the equipment in large facilities such as those dedicated to uranium isotopic enrichment, uranium/plutonium scrap recovery or various stages of fuel fabrication is extensive, the total holdup may be large by its distribution alone, even if deposit thicknesses are small. Good accountability practices require that the measurement uncertainties be as small as possible. This paper describes new analysis procedures for use with traditional holdup analysis methods based on gamma-ray spectroscopy. The new procedures reduce bias that is inherent in traditional measurements of holdup.

The gamma-ray techniques have several advantages over neutron techniques in measurements of holdup. Because gamma rays can be collimated relatively easily, the locations and distributions of deposits can be defined by these measurements. Collimation of the measured radiation also allows deposits to be quantified independent of nearby (larger or smaller) deposits. Gamma-ray detectors can be shielded on the backs and sides to reduce the otherwise large signal from room-background radiation, whose contribution must be subtracted from the total signal to obtain that of the deposit. The photoelectric gamma-ray peaks that are used to quantify holdup deposits can also be used to confirm the identities of the isotopes. Multiple isotopes and elements can be measured independently and simultaneously by choosing the detector and peaks appropriately. Shielded gamma-ray detectors and the required electronics can be small, light in weight, and portable so that measurements can be performed in locations that are difficult to access. Neutron detection methods have few of these advantages.

There are two major shortcomings of gamma-ray techniques for measurements of holdup. (1) One of these represents an area of strength for neutron measurements. Neutrons readily penetrate most processing equipment and are relatively insensitive to self-attenuation effects. Self-attenuation effects (the effects of equipment attenuation are normally addressed in routine holdup measurements) limit the accuracy of holdup measurements performed with gamma rays, and give rise to a negative bias in the holdup assay. (2) Additional limitations in the accuracy of holdup measurements come from model-dependent systematic effects. For many years, geometric models have been used to quantify holdup measured by gamma-ray spectroscopy with collimated detectors. The models themselves give rise to a systematic negative bias in the assay results because the finite geometry of any real deposit does not conform strictly to the geometric model. These are referred to as the finite-source effects.

The new procedures correct for the bias that arises from the systematic effects of both the geometric models and gamma-ray self-attenuation, the two important sources of negative bias in holdup measurements. The procedures used to correct for both of these effects apply to the generalized geometries and rely on a common empirical parameter that self-consistently limits the total error incurred (from uncertain knowledge of this parameter) in the combined correction process.

Section II of this paper reviews the procedures for determining the specific isotopic mass of nuclear material holdup deposits using the Generalized Geometry Holdup (GGH) assay method with portable gamma-ray spectroscopy. Section III summarizes the method that is used to correct the specific isotope mass for the negative

bias caused by equipment attenuation. Section IV describes the new analysis that is used to correct the specific isotope mass for the negative bias caused by finite source dimensions. A six-step process is defined for implementing these new finite-source corrections under the GGH method. Section V describes the new analysis that is used to correct the specific isotope mass for the negative bias caused by gamma-ray self-attenuation. A six-step process is defined for implementing these new self-attenuation corrections under the GGH method. In Section VI, the method of obtaining the total isotope mass from the numerous individual results for specific isotope mass is described. The procedures presented in Sections II–VI represent the complete and correctly ordered sequence of steps for the quantitative analysis of holdup under the GGH method.

Section VII examines the sensitivity of the experimental result for specific isotope mass to the uncertainty in the empirical geometric parameter used to perform the corrections for finite-source and self-attenuation effects. Automated implementation of the new finite-source and self-attenuation corrections under the GGH method is described in Section VIII. Improved detector performance as a means for improving the accuracy of a holdup measurement is summarized in Section IX.

II. GENERALIZED GEOMETRY HOLDUP (GGH) ASSAY METHOD

A. Assumptions and Constraints

The GGH assay method was developed to simplify the quantitative analysis of holdup measurements performed using portable gamma-ray spectroscopy. For these discussions, examples will be taken from data obtained with NaI(Tl)/photomultiplier-tube detectors, which have relatively poor energy resolution. The added benefits of improved energy resolution are addressed in Section IX.

One extreme viewpoint is that the geometry of each individual holdup deposit is unique. Holdup exists in all process equipment regardless of design, size, and shape. Because holdup is measured with portable radiation detectors, variable measurement geometry adds another dimension to the geometric variability of a holdup measurement. The changing radiation environment of each deposit location is yet another. Therefore, the analysis of holdup data, which necessarily involves many measurements (hundreds and, often, thousands), is only practical with geometric constraints on the variables. Four of these constraints were first defined in regulatory guides published by the Nuclear Regulatory Commission approximately 25 years ago and revised at Los Alamos approximately 15 years ago.[1,2]

Two of the four constraints are achieved mechanically.

1. Radiation shielding is used on the back and sides of the crystal so that only radiation impinging on the front of the crystal is detected efficiently.
2. A cylindrical collimator that is concentric with the crystal is installed on the front of the crystal to better define the field of view and maintain a response that is symmetric about the detector axis.

The other two requirements address the measurement geometry.

3. The detector is positioned relative to the deposit so that the spatial distribution of the deposit in its field of view can be described as one of the following with respect to the field of view:
   a. a small point at its center.

b. a narrow, uniform line through its center whose length exceeds its width.
c. a uniform distribution that fills it.

4. Each measurement is performed with an associated, known measurement distance *r* between the detector (crystal) and the deposit.

Figure 1 is a sketch that illustrates the four constraints for the case of a point source.

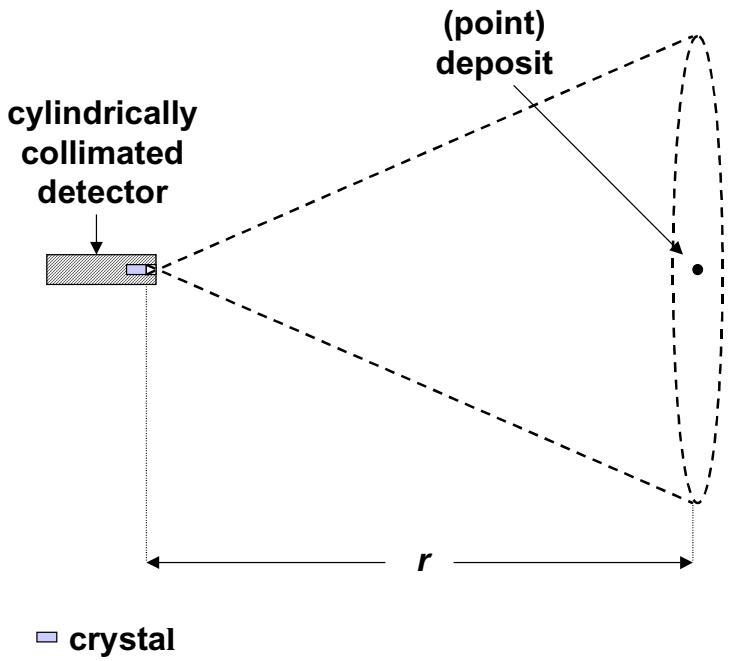

Fig. 1. A point source is positioned on the axis of the cylindrically collimated detector at distance r from the crystal. The field of view (dashed circle) is in the source plane perpendicular to the axis.

A fifth, new constraint is the need to define one additional, empirical parameter associated with the measurement geometry in order to perform the new corrections for finite source dimensions and gamma-ray self-attenuation. This requirement will be discussed in depth in Sections IV and V.

B. Calibration

Calibration of the quantitative assay of a point, line, or area deposit of a given isotope is accomplished with a single reference point source with known self-attenuation. The isotope reference mass m_0 is corrected for self-attenuation before it is applied in the calibration.[3] The response for each gamma-ray peak is measured with this source positioned on the detector axis at a known distance r_0 from the crystal. Measurements are also performed with the source displaced at fixed intervals from the axial position on a line that is perpendicular to it. These data are used to obtain the two-dimensional radial response of the collimated detector. Because the collimation is cylindrical, very few measurements are needed to determine the radial response.

Figure 2 illustrates nine off-axis positions for the point source that can be used to determine the two-dimensional radial response of the collimated detector at the fixed distance. The axial position is at the center of nine concentric circles that intersect each of the nine measurement points indicated with integers. For the fixed measurement distance, the response of the detector to a source at any point on the circle equals the corresponding measured response because of rotational symmetry.

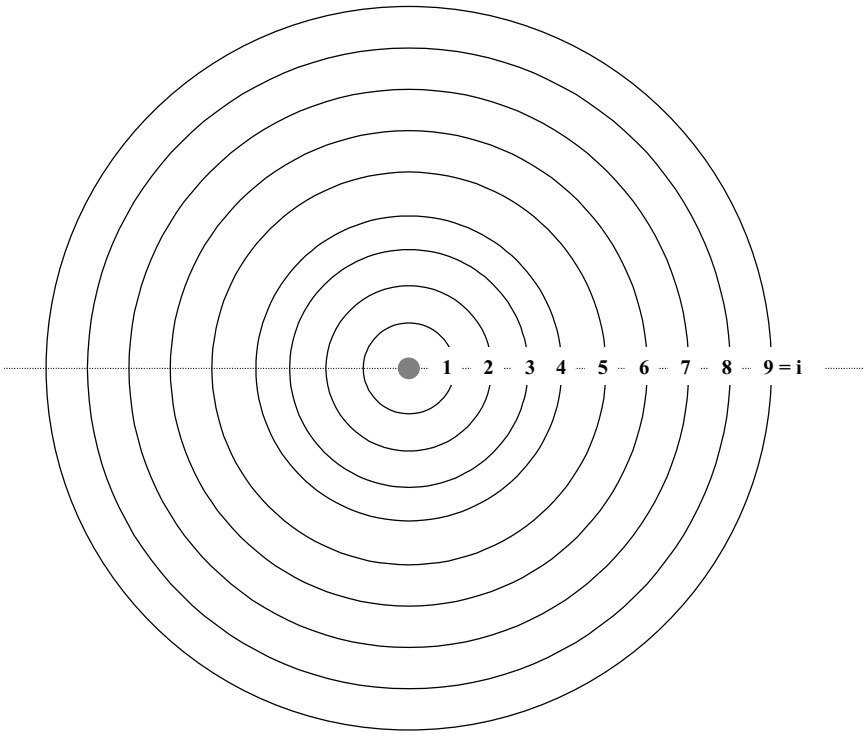

Fig. 2. Nine, equally spaced off-axis positions of the point reference source that can be used to measure the two-dimensional radial response of the gamma-ray detector at a fixed distance r are illustrated. The axial position (center) is the source position illustrated in Fig. 1. The detector response is constant on each concentric circle. Because of radial symmetry, the two-dimensional response can be determined with a small number of measurements.

Figure 3 shows the normalized radial response data (room-background-subtracted, net peak count rate C_i vs axial displacement i of the reference source) obtained for the 414-keV gamma ray of ^{239}Pu in this way using a 2.54-cm-diameter by 5-cm-thick NaI(Tl) detector. The length and diameter of the collimator are both 2.54 cm. The distance between the calibration source and crystal, r_0, is 40 cm. In this example, data were obtained with the point source positioned on both sides of the axial position.

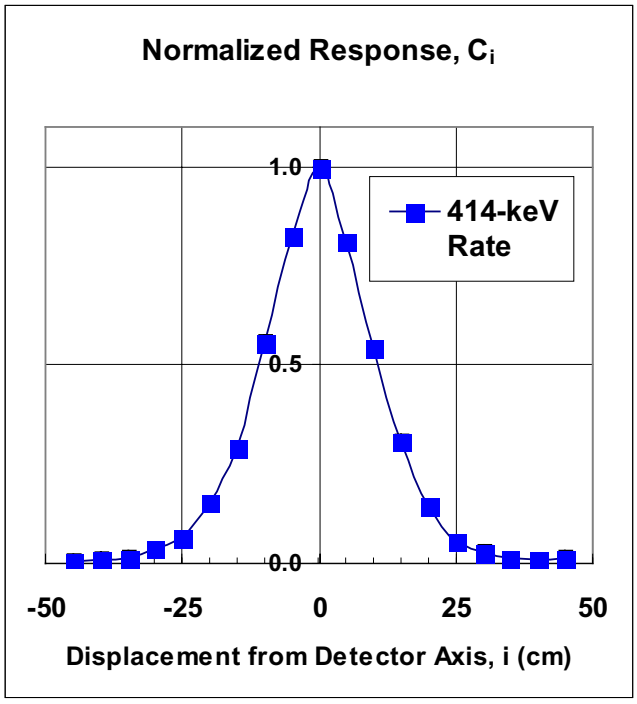

Fig. 3. The normalized net, room-background-subtracted count rate of the ^{239}Pu 414-keV gamma-ray peak vs displacement of the point reference source from the detector axis. A smooth curve connects the data points. This one-dimensional radial response was measured at a distance r_0 of 40 cm with a collimated NaI(Tl) detector (2.54-cm-diameter by 5-cm-thick crystal). The collimator width and diameter were both 2.54 cm. Data obtained on both the right and left sides of the detector axis (positive and negative displacements, respectively, from the detector axis) confirm the radial symmetry.

The data in Fig. 3 are used to obtain the calibration of the quantitative determination (assay) of specific isotope mass in a point, line, or area deposit. The point calibration uses only the un-normalized axial response C_0 (s^{-1}) because the geometric model assumes that a point deposit has no finite width in either dimension of the detector's two-dimensional field of view. The point calibration constant is

$$K_P\ (g \bullet s \bullet cm^{-2}) = m_0 \div (C_0 \bullet r_0^2) \quad . \tag{1}$$

The specific mass of the isotope measured with this detector at a distance r (to obtain a room-background-subtracted net count rate C for the assay peak) and assayed as a point deposit depends on the square of the measurement distance:

$$m_P\ (g) = K_P \bullet C \bullet r^2 \quad . \tag{2}$$

For a point deposit, the specific mass is the measured mass. The random relative uncertainty in the mass, assuming only a random error in C, is

$$\sigma_R(m_P) = \sigma_R(C) \quad , \tag{3}$$

where the relative uncertainty in C, $\sigma_R(C)$, is a random uncertainty propagated from counting statistics.[3]

The line calibration uses both the un-normalized axial response C_0 (s^{-1}) and a geometric parameter L that is evaluated from a sum of the normalized radial responses Ci weighted by the distance between the measurement positions.[3–5] The geometric model assumes that the length of a line deposit exceeds the width of the detector's field of view

and has no finite width in the second dimension of the detector's two-dimensional field of view. The line calibration constant is

$$K_L \text{ (g} \bullet \text{ s} \bullet \text{cm}^{-2}) = m_0 \div (L \bullet C_0 \bullet r_0) \quad . \tag{4}$$

The specific mass of the isotope measured with this detector at a distance r (to obtain a room-background-subtracted net count rate C for the assay peak) and assayed as a line deposit depends on the measurement distance to the first power:

$$m_L \text{ (g/cm)} = K_L \bullet C \bullet r \quad . \tag{5}$$

This is also called the measured linear density of the deposit. The random relative uncertainty in the linear density, assuming only a random error in C is

$$\sigma_R(m_L) = \sigma_R(C) \quad , \tag{6}$$

where the random relative uncertainty in C, $\sigma_R(C)$, is propagated from counting statistics.[3]

The area calibration uses both the un-normalized axial response C_0 (s^{-1}) and a geometric parameter A that is evaluated from a sum of the normalized radial responses Ci weighted by the area between the axially concentric circles that intersect the measurement positions.[3-5] The geometric model assumes that the length and width of an area deposit exceeds the length and width of the detector's two-dimensional field of view. The area calibration constant is

$$K_A \text{ (g} \bullet \text{ s} \bullet \text{cm}^{-2}) = m_0 \div (A \bullet C_0) \quad . \tag{7}$$

The specific mass of the isotope measured with this detector at a distance r (to obtain a room-background-subtracted net count rate C for the assay peak) and assayed as an area deposit is independent of the measurement distance:

$$m_A \text{ (g/cm}^2) = K_A \bullet C \quad . \tag{8}$$

This is also called the measured areal density of the deposit. The random relative uncertainty in the areal density, assuming only a random error in C is

$$\sigma_R(m_A) = \sigma_R(C) \quad , \tag{9}$$

where the random relative uncertainty in C, $\sigma_R(C)$, is propagated from counting statistics.[3]

By adhering to the four constraints listed above, calibration for a breadth of deposit geometries is accomplished simply with only a point isotopic reference source. The great difficulty of fabricating reference samples of special nuclear materials in special geometric distributions is avoided.

C. Performing the GGH Measurement and Assay

Using the GGH assay method to determine quantities of uranium or plutonium holdup by portable gamma-ray spectroscopy requires a portable spectroscopy system and a gamma-ray detector that is equipped and calibrated as described above. A user must understand the assumptions about the point, line, and area geometries in the GGH model in order to make the best choices for positioning the collimated detector for the measurement of each holdup deposit. The distance r between deposit and detector must be recorded for each measurement.

A spectrum of the room background is also required for each measurement. This is particularly important for ^{239}Pu measurements because the 414-keV gamma rays penetrate the detector shield more readily than the 186-keV gamma rays of ^{235}U.

Analysis of the gamma-ray spectra of both the holdup deposit and room background gives a net count rate for the assay peak. Subtraction of the two rates gives the background-subtracted net rate C. This is used along with r and the GGH calibration constants described above to obtain the specific isotope mass for point, line, or area deposits using Eqs. (2), (5), or (8), respectively. The relative uncertainty in the specific mass is determined for each result from Eqs. (3), (6), or (9), respectively.

Because count times are normally very short (5–15 s) in order to perform measurements at as many locations as possible, the random uncertainty can be large for the individual measurements. Propagating the uncertainties of the many measurements that are normally performed to get the total holdup in an extended piece of equipment reduces the relative random error considerably. However, the random uncertainty of an individual measurement must be retained both to propagate this uncertainty and to use in the tests performed to support the self-attenuation corrections described in Section V.

The initial quantitative analysis result is the specific mass m_P (g), m_L (g/cm), or m_A (g/cm^2) for a point, line or area deposit, respectively. Each deposit is measured and analyzed as one of three generalized geometries. Each analysis includes subtraction of the room background signal. However, three additional corrections are required to improve the accuracy of every measurement result. Each contributes to a negative bias in the holdup assay if ignored. The first is the correction for the effects of equipment attenuation. This correction has been carried out routinely for many years. The approach is reviewed briefly in Section III because it is this result that must be corrected further for two effects that have been ignored in GGH measurements in the past. The two new corrections, for the effects of finite source dimensions and self-attenuation, are treated in depth in Sections IV and V. They must be performed in the sequence in which they are treated in this paper.

III. CORRECT THE SPECIFIC MASS FOR EQUIPMENT ATTENUATION

The specific mass of a point, line, or area deposit, m_P (g), m_L (g/cm), or m_A (g/cm^2) is corrected for equipment attenuation effects to get $m_{P,EQ}$ (g), $m_{L,EQ}$ (g/cm), or $m_{A,EQ}$ (g/cm^2) for a point, line, or area source. The correction factor for equipment attenuation is always greater than 1. It is obtained by using the formula

$$CF_{EQ}(Z, E\gamma) = e^{\mu\rho t} \quad , \tag{10}$$

where ρ (g/cm^3) and t (cm) are the density and thickness of the equipment. The mass attenuation coefficient μ is dependent on the Z of the equipment and on the gamma-ray energy E_γ. The correction for equipment attenuation is applied linearly to the room-background-subtracted specific mass of a point, line or area deposit, Eq. (2), (5), or (8), respectively. The corrected specific masses are

$$m_{P,EQ}\,(\mathrm{g}) = m_P \bullet CF_{EQ}(Z,\, E\gamma) \quad , \tag{11}$$

$$m_{L,EQ}\,(\mathrm{g/cm}) = m_L \bullet CF_{EQ}(Z,\, E\gamma) \quad , \tag{12}$$

and

$$m_{A,EQ}\,(\mathrm{g/cm^2}) = m_A \bullet CF_{EQ}(Z,\, E\gamma) \quad , \tag{13}$$

respectively. Because the correction is applied linearly to the uncorrected specific masses, the relative uncertainties in $m_{P,EQ}$, $m_{L,EQ}$ or $m_{A,EQ}$ are unchanged from those given in Eqs. (3), (6) and (9), respectively.

For the assay of ^{239}Pu holdup, $E\gamma$ is usually 414 keV. Because this is higher in energy than 186-keV gamma ray used to assay ^{235}U holdup, the 414 keV is more penetrating of the process equipment. Therefore, for the same type of equipment, the primary equipment-attenuation correction factors for ^{239}Pu holdup measurements will be closer to 1 than those for ^{235}U holdup measurements. However, the equipment is typically not the same because most holdup measurements of ^{239}Pu are performed on equipment that is inside a glove box, which introduces an additional attenuation effect.

Net room-background count rates may require correction for equipment attenuation before being subtracted from the net count rates of the deposits. This occurs when the equipment that contains the deposit shields the detector from room background that reaches the detector through the collimator when the deposit is being measured. When the room background is being measured, the detector may be displaced from this equipment. In this case, the correction factor that must be applied to the net room background rate is the inverse of that obtained in Eq. (10) and is less than 1.

A lack of knowledge of the process equipment affects the accuracy of equipment attenuation corrections. In some cases, the process equipment may not be visible. In others, the distribution of deposits on surfaces of complex equipment may be unknown, and because of the complexity of the equipment it is often difficult to judge its thickness dimension x. In all cases, estimation of the type of material in the equipment and its thickness is recommended. If no correction for equipment attenuation is performed, the individual and total holdup assay results will always be biased low. While a bias of 10% percent is generally not important for an individual deposit, a 10% bias in the total holdup is a serious problem. An estimate of the equipment attenuation effects based on the best information available will give a result that may sometimes be high or low for the individual measurements, but the overall result that is based on many measurements tends to be unbiased.

In recent measurements of ^{239}Pu holdup in bulk-processing equipment in glove boxes using the 414-keV gamma ray and the GGH formalism, values of $CF_{EQ}(Z,$ 414 keV) varied from a low of 1.1 (lead-lined gloves) to a high of 6.2 (steel plates on a glove-

box floor). Equipment attenuation corrections are implemented in most holdup measurements.

IV. CORRECT THE SPECIFIC MASS FOR FINITE SOURCE DIMENSIONS

A. Finite Sources in Holdup Measurements

The effect of the finite dimension of a point or line deposit assayed by the GGH method is substantial if the deposit width *w* is not small compared to the detector's field of view at the deposit distance. The finite-source corrections are not used for area deposits, whose dimensions fill the detector's field of view at the measurement distance *r*.

Although the user may choose a measurement distance to minimize the finite-source effect, some situations arise that cause the effects to be large. These include physical barriers that limit this distance. Areas with high room background rates relative to the count rates from holdup deposits, which may be small, also cause measurements to be performed at smaller distances. This is more common for measurements of ^{239}Pu holdup because the 414-keV gamma ray penetrates the detector shield more readily than the 186-keV gamma ray of ^{235}U. Finally, a smaller measurement distance might be required for holdup in closely spaced equipment to avoid collecting spectral data from more than one piece of equipment in a given measurement for cases in which the deposits must be quantified separately.

Figure 4(a) is an example of a holdup measurement in which the measurement distance *r* and field of view are large compared to the width of the deposit in the vertical pipe. Figure 4(b) illustrates a measurement with the same detector at a similar measurement distance. The diameter of the horizontal overhead duct in Fig. 4.b. is four times that of the vertical pipe in Fig. 4.a. Furthermore, adjacent overhead equipment in Fig. 4(b), which may also contain holdup deposits, is in close proximity to the duct being measured. A larger measurement distance may cause deposits from the adjacent ducts to be included in the field of view. At this measurement distance, the horizontal duct appears as a broad line in the detector's somewhat wider field of view whereas the vertical pipe in Fig. 4(a) is a narrow line in a relatively wide field of view. Depending on the width of the actual deposit in the horizontal overhead duct, a large finite-source effect might be expected for the case illustrated in Fig. 4(b) if the deposit is treated as a line source.

4(a) **4(b)**

Fig. 4. (a) A collimated NaI(Tl) detector (described in caption for Fig. 3) is positioned to obtain the gamma-ray spectrum of holdup in the pipe at the location marked by the white, rectangular bar-coded label. At this measurement distance, the vertical pipe appears as a narrow line in the detector's relatively wide field of view. In this case, the finite-source effect on the GGH line-source assay is small. (b) The same detector is positioned at the same measurement distance from a second bar-coded measurement location on a horizontal duct whose diameter is four times that of the vertical pipe in (a). Because of the overhead equipment in close proximity, it may be difficult to use a larger measurement distance without including additional deposits in the field of view. At this measurement distance, the horizontal duct appears as a broad line in the detector's somewhat wider field of view. In this case, the finite-source effect on the GGH line-source assay may be large.

In Fig. 5, a very large overhead duct is measured from below with a portable, collimated germanium (HPGe) detector. The measurement distance for any detector positioned beneath this duct will be comparable to the duct diameter because of limitations of the fixed height of the equipment above the floor. For common ventilation ducts such as these, the duct width is always a significant fraction of the width of the detector's field of view. A large finite-source effect might be expected for this case if the deposit is treated as a line source. The small measurement distance illustrated in Fig. 5 may have been selected to fill the field of view of the collimated detector with the deposit within the duct. Adjusting the measurement geometry to satisfy requirements for the GGH assay of an area deposit eliminates finite-source effects but increases the probability of sampling effects because a smaller fraction of the total deposit is included in the field of view. In general, larger measurement distances will improve the assay result because the effects of sampling, finite source dimensions and positioning uncertainties are minimized. However, the measurement distance must be optimized rather than maximized because the (degrading) effects of deposits in adjacent equipment and the decreasing signal-to-background ratio of the gamma-ray peak are enhanced at greater measurement distances.

Fig. 5. A very large overhead duct is measured from below with a portable, collimated HPGe detector. The measurement distance for any detector positioned beneath this duct will be comparable to the duct diameter because of the limited height of the equipment above the floor. For common ventilation ducts such as these, the duct width is always a significant fraction of the width of the field of view of the collimated gamma-ray detector. In this case, the duct surface completely fills the field of view of the collimated detector, a geometry that should be (depending on the dimensions of the deposit) best-suited to the GGH assay of an area deposit.

The correction for the finite source dimension of a point, line, or area deposit is applied linearly to the respective specific mass, Eqs. (11), (12), or (13), that has been corrected for equipment attenuation. The correction factor for a finite-source effect is always 1 or greater. The respective specific masses corrected for finite-source effects are

$$m_{P,FIN}\,(\mathrm{g}) = m_{P,EQ} \bullet CF_{FIN,P} \quad , \tag{14}$$

$$m_{L,FIN}\,(\mathrm{g/cm}) = m_{L,EQ} \bullet CF_{FIN,L} \quad , \tag{15}$$

and

$$m_{A,FIN}\,(\mathrm{g/cm^2}) = m_{A,EQ} \tag{16}$$

because

$$CF_{FIN,\mathrm{A}} = 1 \quad . \tag{17}$$

Because the finite-source correction is applied linearly to the specific masses, the relative uncertainties in $m_{P,FIN}$, $m_{L,FIN}$ or $m_{A,FIN}$ are unchanged from those given in Eqs. (3), (6), and (9), respectively.

B. Concept of a Finite Source

Figures 6–8 are sketches that illustrate finite area, line, and point deposits with diagonal shading. The illustrated shading is uniform, unlike most deposits. However, deposit nonuniformity as a departure from the assumptions of the model has a random effect on the result of each holdup measurement. Because hundreds or thousands of individual measurements must be performed for each holdup campaign, a bias is not incurred in the total measured holdup if such nonuniformities are ignored in the analysis of the holdup data.

Like the systematic effects of equipment attenuation, those of finite-source effects cause a negative bias in each individual holdup measurement. If finite-source effects are ignored in the analysis of the holdup data, the total measured holdup will also be biased low. Controls may be implemented to minimize the effects of finite source dimensions by choosing the largest practical measurement distance *r*. While a bias of several percent is generally not important for an individual measurement point out of hundreds or thousands, a several-percent bias in a facility's total holdup can be a serious problem.

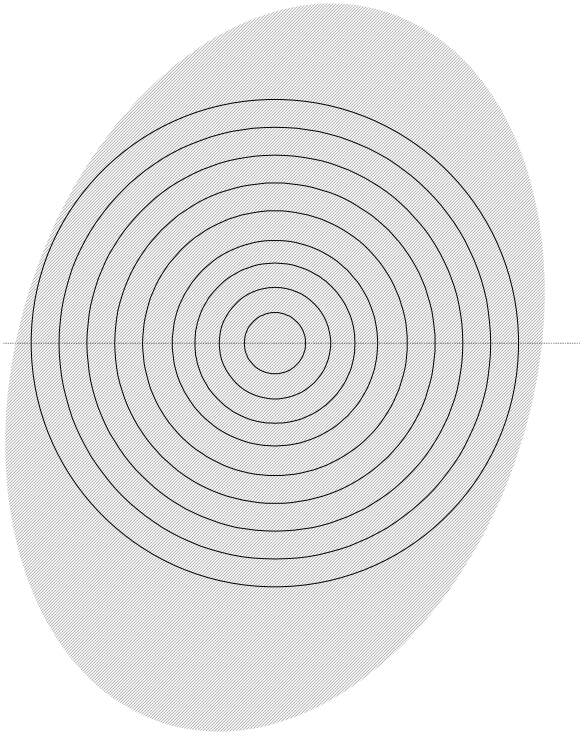

Fig. 6. The large shaded area represents a finite area deposit. It is superimposed on the field of view of the cylindrically collimated detector. The concentric circles represent the equally spaced loci of constant response. The radial positions defined by these circles represent the measurement positions used to obtain the radial response plotted in one dimension in Fig. 3. The finite area deposit fills the field of view in two dimensions, as prescribed by the generalized two-dimensional model for the area source.

The finite area deposit (Fig. 6) fills the field of view of the detector, in accord with the two-dimensional model for the area source. Therefore, the GGH model does not introduce a bias for the finite area source.

The finite line deposit (Fig. 7) is centered in the detector's circular field of view and its length exceeds the width of the field of view, as required by the line source model. However, although its width, *w*, is less than the width of the field of view, it is a considerable fraction of it. The line-source model for GGH assumes that the line width is very small compared to the width of the field of view, as illustrated by the narrow, solid, horizontal line. If the response of the detector to a source at any position on the line deposit is less than the peak of the response at the horizontal displacement (from the axial position), a model-dependent negative bias is incurred. The wider shaded line in Fig. 7 and most line deposits of holdup have finite widths, in this sense. Assuming that the concentric circles in Fig. 7 correspond to the measurement positions in Fig. 3, the detector response varies from ~80–100 % of its 'peak' across the width (*w*, the vertical dimension labeled in Fig. 7) of the wider shaded line. On average for this example, the response to the uniform line is ~90% of the expectation of the model in one of the two dimensions. If the GGH assay of a line is applied in this measurement geometry, the result would be biased low by ~10%. A correction factor of ~0.9^{-1} or 1.11 is required.

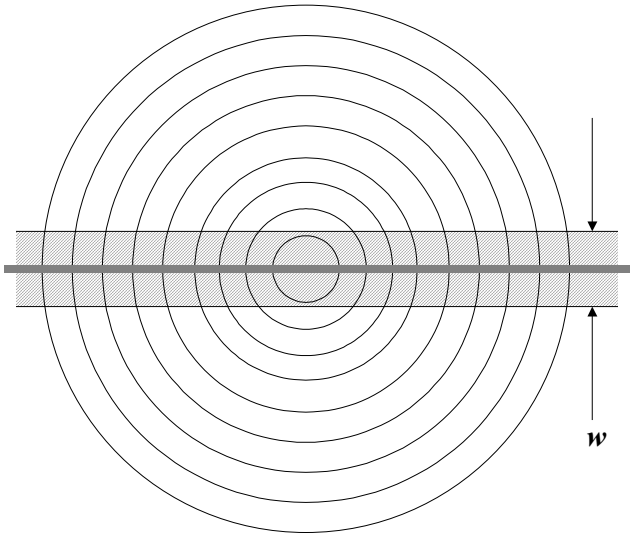

Fig. 7. The wider shaded line represents a finite line deposit. It is superimposed on the field of view of the cylindrically collimated detector. The concentric circles represent the equally spaced loci of constant response. The radial positions defined by these circles represent the measurement positions used to obtain the radial response plotted in one dimension in Fig. 3. The finite line deposit is centered in the field of view with a length that exceeds its width in one dimension, as prescribed by the two-dimensional model for the line source. Its finite width, w, exceeds that prescribed by the model in one dimension and illustrated by the narrow, solid line.

The finite point deposit (Fig. 8) is centered in the circular field of view, as required by the point-source model. Although the width, *w*, of the larger shaded area (finite point deposit) is less than the width of the field of view in Fig. 8, it is a considerable fraction of it. The point-source model for GGH assumes that the point width is very small compared to the width of the field of view, as illustrated by the smaller, solid point. If the response of the detector to a source at any position on the point deposit is less than the peak of the response at the center of the field of view, a model-dependent negative bias is incurred. The larger shaded point in Fig. 8 and most point deposits of holdup have finite widths, in this sense. Assuming that the concentric circles in Fig. 8 correspond to the measurement positions in Fig. 3, the detector response varies from

~80–100 % of its 'peak' across both (vertical and horizontal) width dimensions of the diagonally shaded point in Fig. 8. On average for this example, the response is ~90% of the expectation of the model in both of the two dimensions. If the GGH assay of a point is applied in this measurement geometry (note that the width, *w*, of the finite point in Fig. 8 is the same as that of the finite line in Fig. 7), the result would also biased low, but by ~20% in the case of the point source. A correction factor of $\sim 0.9^{-2}$ or 1.23 is required. The point-source correction factor is the square of that for the line source because the model constrains the geometry of the point deposit in two dimensions rather than one.

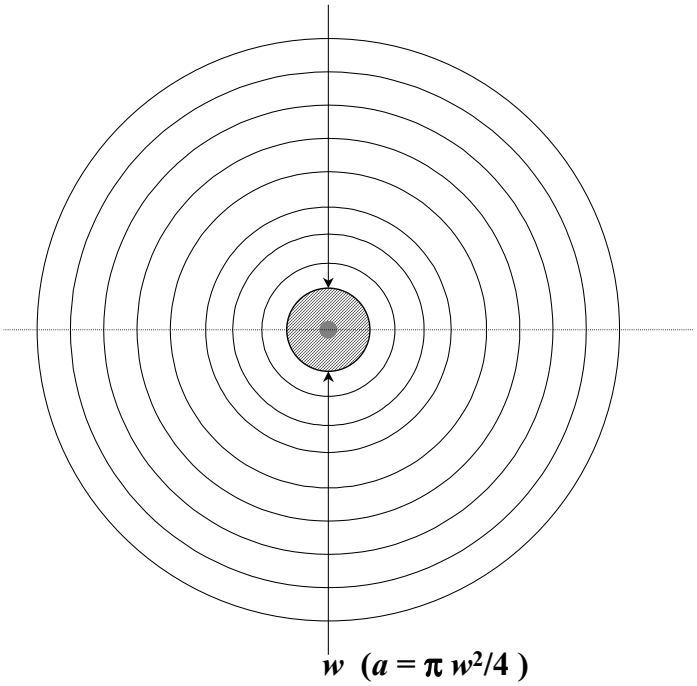

Fig. 8. The larger shaded area represents a finite point deposit. It is superimposed on the field of view of the cylindrically collimated detector. The concentric circles represent the equally spaced loci of constant response. The intersections of the circles with a diameter are the measurement positions used to get the one-dimensional radial response plotted in Fig. 3. The finite point deposit is centered in the field of view, as prescribed by the two-dimensional model for the point source. Its finite width w (which determines its area a) exceeds that prescribed by the model in two dimensions (illustrated by the small, solid point).

C. Correcting a Measured Holdup Deposit for Finite Source Dimensions

Correcting for the finite dimension of a deposit begins with a decision on the width *w* of the deposit. An over- or under-estimate of *w* leads to over- or under-correction for the effect of the finite source dimension. However, as described previously, this characteristic is preferable to a persistent negative bias caused by uncorrected finite-source effects because the total holdup will tend to be unbiased. To minimize the magnitude of the over- or under-correction of the individual holdup measurements, the choice of the finite source dimension must be a best estimate based on a knowledge of the equipment and process and, if possible, on a scanning of the gamma-ray count rate across the surface of the equipment with a collimated detector. For example, if a duct is oriented vertically, it may be reasonable to assume that the deposit width is the inner diameter of the duct. If it is horizontal and cylindrical, a scan of the equipment may be a better approach to determining the deposit width.

There is another aspect of *w* that should be addressed at this point in the derivation of the correction algorithms. Knowledge of the same experimental width parameter *w* required for the finite-source corrections is also required in the corrections for self-attenuation, as described in Section V. Section VII will demonstrate that there is

actually a compensating effect between the finite-source and self-attenuation corrections in the sensitivity of the experimental result for specific isotope mass to the uncertainty in the experimental width parameter *w*. Therefore, it is very important to perform both corrections

- to avoid a negative bias in the measured holdup (that results both from the effects of the finite source dimensions and self-attenuation), and
- to reduce the magnitude of the (positive or negative) systematic effects associated with over-/under-estimates of the experimental width parameter *w*.

The corrections for the finite dimensions of a holdup deposit can be performed in six steps. The emphasis is on generality. The procedure is the same for and applicable to all measurements. Previous efforts to address the finite dimensions of deposits have viewed the geometry of the particular type of holdup deposit uniquely in an approach that does not extend generally to other geometries.[6–8] The current emphasis is also on formality and simplicity so that the procedures can be automated by a computer program.

The six steps to finite-source corrections are as follows.

1. Plot the normalized radial response data C_i for the assay gamma ray (the 414-keV ^{239}Pu peak or the 186-keV ^{235}U peak) measured with the point reference source at the positions i along a line at a fixed distance r_0 from a particular detector. Figure 3 shows this plot, with a smooth curve $C(x)$ drawn through the data points, for the ^{239}Pu gamma ray at 414 keV. Alternatively, fit the C_i data to a normalized Gaussian $G(x)$ or another form that represents the shape of the radial response curve.

   $$C(x) = G(x) = \exp[-0.5(2.354x/\mathrm{FWHM})^2] \quad , \tag{18}$$

   where "*x*" is the displacement of the source from the detector axis. Figure 9 is a plot of the fit of Eq. (18) to the data from Fig. 3. The data points are also plotted. The curve $C(x)$ or $G(x)$ is used to obtain all corrections for the finite dimensions of point or line deposits measured with this particular detector.

2. Measure a holdup deposit at distance *r* with finite dimension *w* (width of a line or diameter of a point deposit). The ratio r/r_0 is used to adjust *w* for the difference between *r* and the calibration distance r_0:

   $$w_0 = w \bullet (r/r_0)^{-1} \, . \tag{19}$$

3. Determine the normalized radial response, $C(w_0/2)$, at the outer edge ($x = w_0/2$) of the line or point by reading it from the plot (Fig. 9) or evaluating it from Eq. (18).

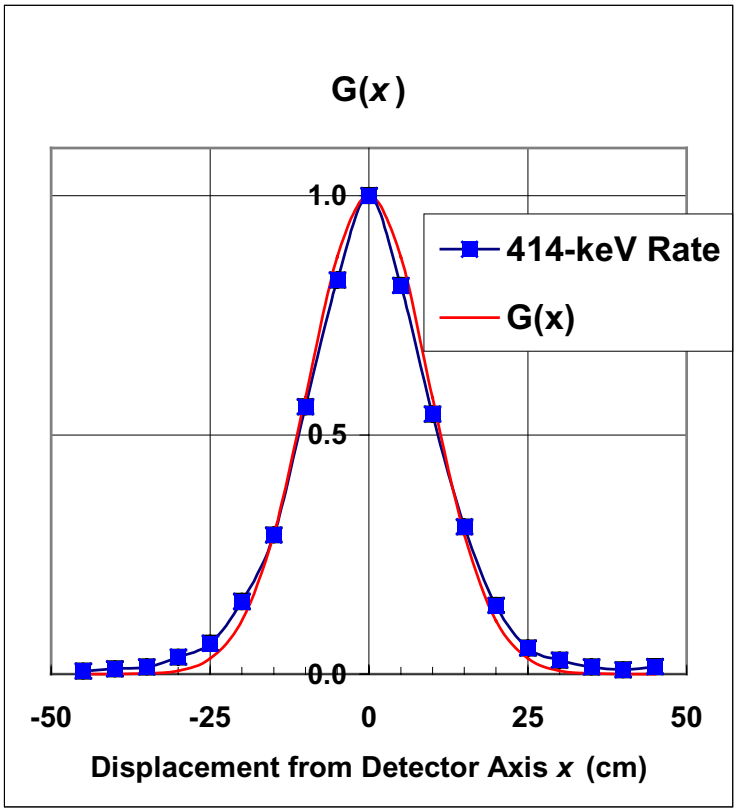

Fig. 9. The data from Fig. 3 (normalized net, room-background-subtracted count rate of the ^{239}Pu 414-keV gamma-ray peak vs displacement of the point reference source from the detector axis) are shown in blue. The measurements were performed at a distance r_0 of 40 cm with a collimated NaI(Tl) detector. The red curve is the fit of Eq (18) (normalized Gaussian) to these data. The full width at half maximum (FWHM) of the fit is 22 cm.

4. Obtain the average of $C(w_0/2)$, the normalized response at the edge of the deposit, and 1, the normalized response at the center of the deposit, to get the effective radial response

$$C_{EFF} = [\ 1 + C(w_0/2)\ ] / 2 \qquad (20)$$

for the source of finite dimensions.

5. Compute the finite-source correction factor for a line deposit

$$CF_{FIN,\,L} = (C_{EFF})^{-1} \quad , \qquad (21)$$

or a point deposit

$$CF_{FIN,\,P} = (C_{EFF})^{-2} \quad . \qquad (22)$$

6. Apply the finite-source correction to the equipment-attenuation corrected specific mass for a point deposit using Eq. (14). Apply the finite-source correction to the equipment-attenuation corrected specific mass for a line deposit using Eq. (15). Recall that the finite dimensions of the area deposit complies with the model for this geometry so that there is no correction to the equipment-attenuation corrected specific mass. See Eq. (16).

The advantages of using an analytical form such as a Gaussian fit to the radial response data C_i (rather than a smooth curve drawn through the data) include greater consistency in implementing the correction, and greater ease of automation. One disadvantage is that the shape of the radial response changes with the energy of the gamma ray for a given detector. Therefore, the analytical form may represent the measured response better at some energies than at others. The Gaussian, for example, gives a much better fit to the radial response that is measured with the lead-collimated compact NaI(Tl) detector (2.54-cm-diameter crystal and collimator) for the ^{235}U gamma ray at 186 keV than for the ^{239}Pu gamma ray at 414 keV (Fig. 9).

A sample calculation showing the effect of a finite-source correction is presented below. It is based on using the detector described in Fig. 9 to measure the 414-keV gamma ray of ^{239}Pu in a 24-cm-wide vertical duct viewed as a (wide) line at r = 80 cm. For r_0 = 40 cm, Eq. 19 gives

$$w_0 = 12 \text{ cm} \quad ,$$

and Eq. 18 (or Fig. 9) gives

$$C(w_0/2) = 0.8 \quad .$$

Therefore, the effective normalized radial response to deposits in the duct (Eq. 20) is

$$C_{EFF} = (1 + 0.8)/2 = 0.9 \quad .$$

The correction factor for the finite source dimension, which multiplies $m_{L,EQ}$ for the finite line deposit (Eq. 15) in this example, is

$$CF_{FIN,\,L} = (0.9)^{-1} = 1.11 \quad .$$

In recent measurements of plutonium holdup[9] in high-throughput bulk-processing equipment inside of glove boxes using the 414-keV gamma ray and the GGH formalism, the values of $CF_{FIN,\,L}$ obtained varied from 1 (for area deposits on glove-box surfaces) to 1.25 (for line deposits of powder accumulated in troughs on the glove-box floor).

The six-step procedure for finite-source corrections described and illustrated above applies to holdup deposits measured with a cylindrically collimated gamma-ray detector of any type. It applies to holdup measurements that are set up and analyzed as point or line deposits under the GGH formalism. Like the GGH procedure itself, the corrections can be implemented for any gamma-ray spectrometer detector (NaI, BGO,

HPGe, CdZnTe, etc.) and any gamma-ray peak chosen for the quantitative analysis. Because of certain choices made during the holdup measurements that are based on the radiological characteristics of ^{235}U and ^{239}Pu, corrections for the effects of finite source dimensions will tend to be larger for measurements of ^{239}Pu than for ^{235}U. This is the case because the 414-keV gamma ray of ^{239}Pu is more penetrating of the background shielding on the detectors than is the 186-keV gamma ray of ^{235}U. Choosing a smaller measurement distance r may be necessary more often for the ^{239}Pu measurements to improve the ratio of signal to background to achieve the required detection sensitivity.

The six-step procedure for finite-source corrections described and illustrated above is currently automated[10] in the stand-alone VisualBasic program *Finite v. 1.0* for testing purposes. This module utilizes the normalized Gaussian form (Eq. 18) for the radial response function $C(x)$. This software module will be incorporated into the next generation of the *HMS3* software, which automates the plant-wide portable measurement and tracking of holdup using the GGH formalism.[11–13] Automation is, in fact, possible because of the simplicity and generality of the approach. The automated implementation of the finite-source corrections in an integrated holdup measurement system is discussed in Section VIII.

V. CORRECT THE SPECIFIC MASS FOR SELF-ATTENUATION EFFECTS

A. Self-Attenuation Effects in Holdup Measurements

Characteristic of bulk quantities of special nuclear materials is the self-absorption of gamma rays emitted by the material. A detailed treatment of these effects[14] includes descriptions of formal experimental methods that can be used to correct for self-attenuation when the quantitative analysis relies on a gamma ray emitted by the material. The corrections are important whenever a quantitative gamma-ray measurement is based on the net counts in a spectral region, which is the case in the GGH approach to measurements of holdup. If the effects are ignored, every measurement result will again (as with equipment-attenuation and finite-source effects) be biased low.

Two approaches that are used routinely in gamma-ray nondestructive assay (NDA) measurements involve determining the (1) intensities of gamma rays transmitted through the material from external (transmission) sources, and (2) relative intensities of multiple gamma rays emitted from the bulk material by a single isotope. Both of these techniques have been explored for holdup measurements, and neither is satisfactory in these applications as described below.

Transmission sources are difficult to use in portable measurements that characteristically lack fixed or well controlled geometries and a good definition/knowledge of the materials (other than the nuclear material deposits) in the transmission path. Implementing the use of transmission sources for holdup measurements is a cumbersome procedure because the implementation of a transmission source hinders the rapid performance of measurements at a large number of locations. There are also safety restrictions on carrying a gamma-ray source of sufficient intensity to perform the transmission measurements at relatively large distances and through dense equipment. Attempts to use transmission sources to obtain corrections for self-attenuation in the measurement of holdup typically lead to systematic biases of 100% or more.[15–16]

Measurements of the relative intensities of multiple gamma rays emitted from the bulk material require the use of HPGe detectors, which are difficult to use for routine measurements of holdup because of the large size and weight of such detectors, especially when fitted with shielding against gamma-ray backgrounds. Efforts to perform such measurements to correct for self-attenuation of gamma rays by the holdup deposits have not been successful.[16] Weak signals that are typical of holdup measurements limit the statistics of the net counts in useful gamma-ray peaks. Very long count times are not practical in these circumstances.

Typical holdup deposits tend to be thin. Therefore, for a given facility, the average self-attenuation effect may be as large as a few percent, depending on the energy of the assay gamma ray. While a bias of several percent is generally not important for an individual measurement point, a several-percent bias in a facility's total holdup is can be serious problem.

The magnitude of the effect of gamma-ray self-attenuation for a measured holdup deposit can be determined if the areal density of the deposit, uncorrected for self-attenuation (but corrected for room background, equipment attenuation, and finite-source effects), is known. Because the atomic numbers (the Zs) of actinides are large and the actinide density dominates the density of the holdup deposit, the actinide areal density is sufficient to perform the correction. The key to obtaining the self-attenuation correction is that the specific mass of the actinide isotope obtained from the holdup measurement can be converted to the uncorrected areal density of the actinide. In the cases of line or point deposits, the conversion requires the experimental width parameter *w*.

The holdup measurement of an area deposit gives the areal density of the actinide isotope directly. This can be readily converted to the areal density of the actinide element using the known isotopic fraction. This in turn is used directly to determine the effect of self-attenuation. The holdup measurement of a line deposit gives the uncorrected linear density of the actinide isotope. This can be converted to an uncorrected areal density by dividing by the experimental width parameter *w* of the line deposit. Subsequently, the effect of gamma-ray self-attenuation for the line deposit is determined as for the area deposit. The holdup measurement of a point deposit gives the uncorrected mass of the actinide isotope. This can be converted to an uncorrected areal density by dividing by the area *a* of the point deposit, which is related simply to the experimental width parameter *w*:

$$a = \pi \bullet (w/2)^2 \quad . \tag{23}$$

Subsequently, the effect of gamma-ray self-attenuation for the point deposit is determined as for the area deposit. The determination of the self-attenuation effect from the measured areal density is described next.

B. Determining the Self-Attenuation Effect from the Measured Areal Density

The areal density of an actinide deposit is its mass per unit area (typically in g/cm^2). The specific mass of a holdup deposit measured under GGH can be used to obtain the measured actinide areal density, $(\rho x)_{MEAS}$, as described in Section V.A. The true areal density, (ρx), is corrected for the effect of self-attenuation on the gamma ray used to

perform the measurement. The correction for self-attenuation is determined from the ratio of the true to the measured areal densities of a slab deposit of the total actinide:

$$(\rho x)/(\rho x)_{MEAS} = \mu(\rho x)/[1-e^{-\mu(\rho x)}] \quad , \tag{24}$$

where μ is the mass attenuation coefficient (in cm^2/g) of the actinide (element, compound, or mixture) at the energy of the gamma ray used to perform the measurement.[14] Rearranging Eq. (24) gives the true areal density (corrected for self-attenuation) as a function of the measured:

$$(\rho x) = - (\ln[1 - \mu(\rho x)_{MEAS}])/\mu \quad . \tag{25}$$

Equation (25) is used to perform the nonlinear conversion of the measured areal density of a total actinide holdup deposit to the result corrected for self-attenuation. Its use requires knowing the mass attenuation coefficient of the actinide deposit. This information is available for any element or for particular compounds or mixtures of elements.[15] A choice of the element or the particular compound or mixture must be made by someone with process knowledge. Because their mass attenuation coefficients μ are so much larger, lower energy gamma rays will have the greatest sensitivity to this choice. Therefore, Eq. (25) is examined for three common forms of uranium deposits (U metal, UO_2 and U_3O_8) for the relatively low-energy 186-keV gamma ray of ^{235}U. Table I lists the μ values for 186-keV gamma rays for these three materials.

Table I.
Gamma-ray Mass Attenuation Coefficients

Material	E_γ (keV)	μ (cm^2/g)
U	186	1.46
UO_2	186	1.30
U_3O_8	186	1.26
Pu	414	0.270
PuO_2	414	0.250

The relationship between (ρx) and $(\rho x)_{MEAS}$ defined by Eq. (25) is plotted for the three materials in Fig. 10. The straight line in each graph of Fig. 10 has a slope of 1. Therefore, the ratio of the ρx values on the curved line to those on the straight line is the correction factor for self-attenuation. For deposit densities at or below 0.3 g/cm^2 (most holdup deposits are in this range), the correction factors for a particular gamma-ray energy are

hardly different for the different materials. Although Fig. 10 shows that this is not the case for the thicker deposits, such deposits are generally not measurable by passive gamma-ray techniques and may be mandated for cleanout.

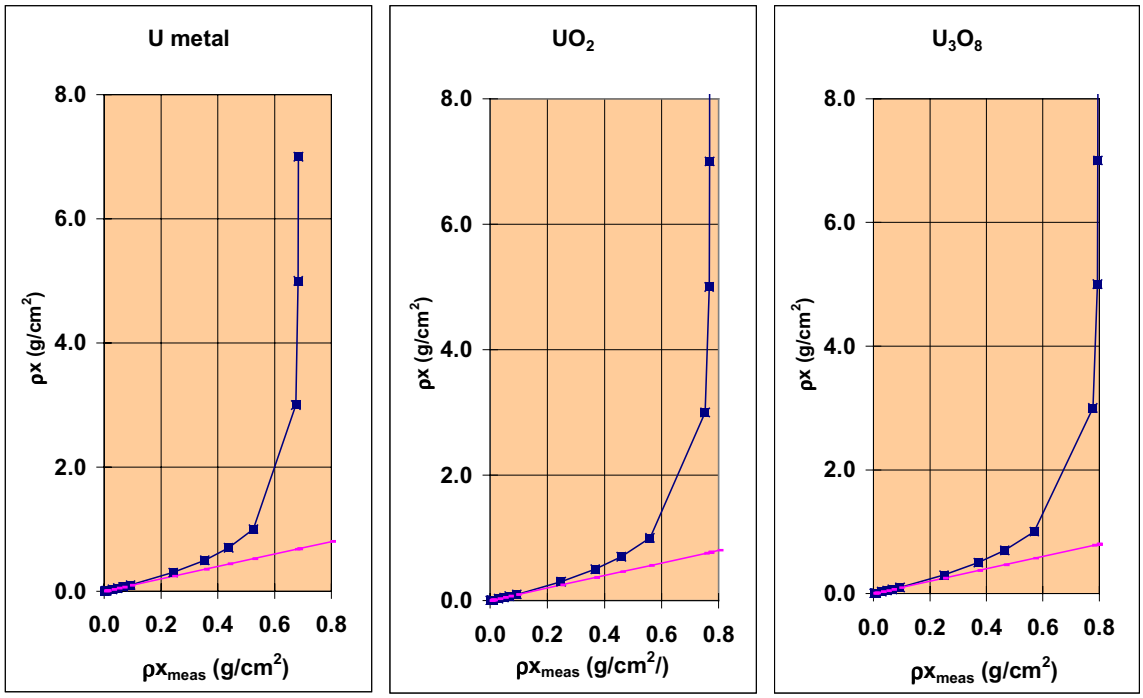

Fig. 10. True vs measured thickness (areal density of uranium, g/cm^2) is plotted for 186-keV gamma-rays from uranium metal, UO_2, and U_3O_8. The data points are determined from Eq. 25. The measured thickness is determined from the holdup specific mass corrected for the effects of room background, equipment attenuation, and finite source dimensions. The straight line has a slope of 1. Therefore, the correction factor for self-attenuation is the ratio of the curved line to the straight line.

Equation (25) shows that the product $\mu(\rho x)_{MEAS}$ must be less than 1. The apparent singularity in each plot in Fig. 10 is the result of the approach of the product $\mu(\rho x)_{MEAS}$ to 1, which corresponds to a deposit that is infinitely thick to its own gamma rays. Deposits near this thickness for a given assay gamma ray cannot be measured by these strictly passive methods. Furthermore, as the product $\mu(\rho x)_{MEAS}$ approaches 1 the uncertainty in the corrected value is magnified relative to the measured uncertainty, as follows:

$$\sigma(\rho x) = \sigma(\rho x)_{MEAS} / [1 - \mu(\rho x)_{MEAS}] \quad , \tag{26}$$

making the corrected results of such measurements unrealistic.

In the case of plant-wide measurements of holdup, the uncertainty in the measured result, $\sigma(\rho x)_{MEAS}$, can be large because the count times tend to be very short. A conservative approach should be implemented primarily for safety reasons to identify those deposits for which the product $\mu(\rho x)_{MEAS}$ is dangerously close to 1, such that the deposit is statistically equivalent to an infinite thickness. For example, reject a measurement for which

$$\mu(\rho x)_{MEAS} + K \bullet \mu \bullet \sigma(\rho x)_{MEAS} \geq 1 \quad , \tag{27}$$

where K is chosen to be three or more. Such measurements cannot be corrected for self-attenuation and must be measured again with improved statistics before employing the corrections. If the remeasured result with improved statistics is rejected by Eq. (27), a cleanout should be considered. Even if the dimensions of the equipment are deemed critically safe, the possibility that the holdup deposit fills the interior cavity of the equipment may raise production concerns. Such deposits certainly cannot be measured by passive gamma-ray techniques. Because most holdup deposits are thin, remeasurement is rarely necessary. When deposits do become too thick to perform reliable self-attenuation corrections, it is reasonable to consider cleanout alternatives for enhanced safety and productivity.

C. Correcting a Measured Holdup Deposit for Self-Attenuation Effects

Correcting for gamma-ray self-attenuation in a holdup deposit also begins with a decision on the width (w) of the deposit, except that this decision has already been made in the previous correction procedure for finite-source effects. An over- or underestimate of w leads to under- or over-correction for the effect of self-attenuation. This is opposite to the result of over- or under-estimating w in the case of the finite-source correction. For this reason, in a limited range of deposit thickness, the effects of errors in the estimates of w tend to compensate for each other when both corrections are performed. This will be described in Section VII.

The corrections for finite source dimensions, like the self-attenuation correction addresses an additional, persistent negative bias that propagates to the total holdup. The correction factor for self-attenuation is always greater than 1. As discussed in the previous correction procedure for finite-source effects, the correction process leads to a total holdup result that will tend to be unbiased, because the correction is sometimes high or low for an individual measurement.

Unlike the previous corrections for equipment attenuation, Eqs. (11–13), and finite-source effects, Eqs. (14–16), the correction for self-attenuation, Eq. (24), is a nonlinear function of the specific mass (converted to areal density) of the deposit. For this reason, it must be applied after all the other corrections have been made. For the same reason of nonlinearity, and because the self-attenuation effect is determined by the areal density of the total actinide deposit, the isotope fraction must be used to convert the measured areal density of the isotope to that of the element if only one actinide is present. If more than one actinide is present in significant amounts, both the element and isotope fractions are multiplied for use in the conversion step.

The relative uncertainty in the specific mass corrected for equipment attenuation and finite source dimensions of a point, line or area deposit remained unchanged from the respective uncorrected values, Eqs. (3), (6), or (9), because the corrections were linear. The areal density (and, therefore, specific mass) corrected for self-attenuation using Eq. (25) varies nonlinearly with the deposit thickness. Therefore, Eq. (26) must be used to determine the propagated relative uncertainty in the specific mass of a (point, line, or area) deposit corrected for self-attenuation.

The correction for self-attenuation of gamma rays by a holdup deposit can be performed in six steps. The emphasis is on generality. The procedure is the same for and applicable to all measurements, which is unlike previous efforts to address the effects of

self-attenuation in holdup measurements.[15–16] The emphasis is also on formality and simplicity, which enable automated use of the procedures.

The six steps to self-attenuation corrections are as follows.

1. Convert the specific isotope mass of a point, line or area source obtained in Eqs. (14–16), respectively, to the specific actinide (AC) mass as follows:

   $$m_{P,FIN\,AC}\,(\mathrm{g}) = m_{P,FIN} / \varepsilon \quad , \tag{28}$$

   $$m_{L,FIN\,AC}\,(\mathrm{g/cm}) = m_{L,FIN} / \varepsilon \quad , \tag{29}$$

   and

   $$m_{A,FIN\,AC}\,(\mathrm{g/cm^2}) = m_{A,FIN} / \varepsilon \quad . \tag{30}$$

   The parameter, ε, is the product

   $$\varepsilon = f_I \bullet f_E \quad , \tag{31}$$

   where f_I is the fraction of the actinide isotope relative to the element total and f_E is the fraction of the element relative to the actinide total. (For a single-element actinide deposit, f_E is 1.)

2. Convert the specific actinide mass to the measured actinide areal density $(\rho x)_{MEAS}$ as follows.

   (a) For a point deposit

   $$(\rho x)_{MEAS,P}\,(\mathrm{g/cm^2}) = m_{P,FIN\,AC} / a \quad . \tag{32}$$

   (b) For a line deposit

   $$(\rho x)_{MEAS,L}\,(\mathrm{g/cm^2}) = m_{L,FIN\,AC} / w \quad . \tag{33}$$

   (c) For an area deposit

   $$(\rho x)_{MEAS,A}\,(\mathrm{g/cm^2}) = m_{A,FIN\,AC} \quad . \tag{34}$$

   Here, w (in cm) is the finite width of the line (or point) deposit, and a (in $\mathrm{cm^2}$) is the area of the point deposit, as defined in Eq. (23).

3. Use this measured actinide areal density of a point, line, or area deposit to test if it is in a range that is valid for self-attenuation corrections. Recall that the true areal density ρx cannot be determined

if the measured value is so large that $\mu(\rho x)_{MEAS}$ approaches 1. The relative uncertainties in the values of $(\rho x)_{MEAS,P}$, $(\rho x)_{MEAS,L}$, and $(\rho x)_{MEAS,A}$ are the respective relative uncertainties $\sigma_R(m_P)$, $\sigma_R(m_L)$, and $\sigma_R(m_A)$ determined from Eqs. (3), (6), and (9). This is because all conversions and corrections have been applied linearly. Using these uncertainties, the following tests (or equivalent alternatives) can be implemented. (If a test fails, remeasure the deposit with improved statistics and retest, or consider a cleanout of the equipment.) If

$$\mu(\rho x)_{MEAS,P} + 3 \bullet \mu \bullet [\sigma_R(m_P)] \bullet (\rho x)_{MEAS,P} < 1 \quad , \tag{35}$$

or

$$\mu(\rho x)_{MEAS,L} + 3 \bullet \mu \bullet [\sigma_R(m_L)] \bullet (\rho x)_{MEAS,L} < 1 \quad , \tag{36}$$

or

$$\mu(\rho x)_{MEAS,A} + 3 \bullet \mu \bullet [\sigma_R(m_A)] \bullet (\rho x)_{MEAS,A} < 1 \tag{37}$$

for a point, line, or area deposit, respectively, proceed with the self-attenuation corrections. In some cases, an approach that is more conservative than these tests may be required. Holdup deposits normally do not approach infinite thickness, so failures of these tests will be infrequent, but procedures must address this possibility.

4. Use the relationship of Eq. (25) and the measured actinide areal density of a point, line, or area deposit to obtain the respective areal density of a point, line, or area deposit corrected for self-attenuation:

$$(\rho x)_P = -(1/\mu) \bullet \ln[1 - \mu(\rho x)_{MEAS,P}] \quad , \tag{38}$$

$$(\rho x)_L = -(1/\mu) \bullet \ln[1 - \mu(\rho x)_{MEAS,L}] \quad , \tag{39}$$

and

$$(\rho x)_A = -(1/\mu) \bullet \ln[1 - \mu(\rho x)_{MEAS,A}] \quad . \tag{40}$$

Note that the correction for self-attenuation is independent of deposit type because the specific mass, whose dimensions are geometry-dependent, has been converted to areal density for all deposit geometries. The absolute uncertainties in the corrected areal densities $(\rho x)_P$, $(\rho x)_L$, and $(\rho x)_A$ are determined using Eq. (26) as follows:

$$\sigma(\rho x)_P = [\sigma_R(m_P) \bullet (\rho x)_{MEAS,P}] / [1 - \mu(\rho x)_{MEAS,P}] \quad , \tag{41}$$

$$\sigma(\rho x)_L = [\sigma_R(m_L) \bullet (\rho x)_{MEAS,L}] / [1 - \mu(\rho x)_{MEAS,L}] \quad , \tag{42}$$

and

$$\sigma(\rho x)_A = [\sigma_R(m_A) \bullet (\rho x)_{MEAS,A}] / [1 - \mu(\rho x)_{MEAS,A}] \quad . \tag{43}$$

Typically, a test of relative uncertainty in the corrected areal density is justified at this point because the denominator in Eqs. (41–43) magnifies it compared to the relative uncertainty in the uncorrected areal density. An upper limit, F, that is less than 1 (0.5, for example) may be chosen for the test, such that if

$$\sigma(\rho x)_P / (\rho x)_P > F \quad , \tag{44}$$

or

$$\sigma(\rho x)_L / (\rho x)_L > F \quad , \tag{45}$$

or

$$\sigma(\rho x)_A / (\rho x)_A > F \quad , \tag{46}$$

a remeasurement of the deposit with improved statistics followed by a repeat of this test, Eqs. (44–46), would be recommended.

5. Convert the corrected areal density to the respective specific mass for the point, line, or area actinide deposit, corrected for self-attenuation effects, as follows:

$$m_{P,SELF\,AC}\,(\mathrm{g}) = a \bullet (\rho x)_P \quad , \tag{47}$$

$$m_{L,SELF\,AC}\,(\mathrm{g/cm}) = w \bullet (\rho x)_L \quad , \tag{48}$$

and

$$m_{A,SELF\,AC}\,(\mathrm{g/cm^2}) = (\rho x)_A \quad . \tag{49}$$

6. Convert the self-attenuation corrected specific actinide mass of the point, line, or area deposit to the respective corrected specific isotope mass:

$$m_{P,SELF}\,(\mathrm{g}) = \varepsilon \bullet m_{P,SELF\,AC} \quad , \tag{50}$$

$$m_{L,SELF}\,(\mathrm{g/cm}) = \varepsilon \bullet m_{L,SELF\,AC} \quad , \tag{51}$$

and

$$m_{A,SELF}\ (\mathrm{g/cm^2}) = \varepsilon \bullet m_{A,SELF\ AC} \quad . \tag{52}$$

The relative uncertainties in these three self-attenuation-corrected results for specific isotope mass are unchanged from those given by Eqs. (41–46), respectively.

Although there is little that the measurement practitioner can do to minimize the effects of self-attenuation, administrative controls will generally mandate a cleanout of the process equipment for safety reasons and for optimization of process operation. Such controls are often determined from the measured holdup values. The self-attenuation effects are generally much larger for measurements of ^{235}U holdup that is based on the 186-keV gamma ray than for measurements of ^{239}Pu holdup based on the 414-keV gamma ray for the same elemental deposit thickness. This is because the mass attenuation coefficients are five times larger for the lower energy gamma ray, as indicated in Table I.

In recent measurements of ^{239}Pu holdup in bulk-processing equipment inside of glove boxes using the 414-keV gamma ray and the GGH formalism, the magnitude of the correction for self-attenuation determined by the ratio $(\rho x) / (\rho x)_{MEAS}$, Eq. (24), was as large as 1.11 for powder deposits on the glove-box floor.

The six-step procedure for self-attenuation corrections described and illustrated above is currently automated[7] in the stand-alone VisualBasic program *SelfAttn v. 1.0* for testing purposes. The automation is possible because of the simplicity and generality of the approach. This software module will be incorporated into the next generation of the HMS3 software, which automates the plant-wide portable measurement and tracking of holdup using the GGH formalism.[8–10] Automated implementation of the self-attenuation corrections is discussed in Section VIII.

VI. COMPUTATION OF TOTAL ISOTOPE MASS IN EQUIPMENT

The total isotope mass contained in a piece of equipment is a product of the corrected specific isotope mass that represents the entire equipment and a physical dimension parameter. The parameter is 1 for a point deposit, the equipment length L_{TOT} (in cm) for a line deposit, or the equipment area A_{TOT} (in $\mathrm{cm^2}$) for an area deposit. Frequently, an average of the multiple measurements of corrected specific isotope mass performed at different locations on the equipment will be used to represent the equipment. These average results for point, line, or area deposits are $m_{P,SELF\ AVG}$ (g), $m_{L,SELF\ AVG}$ (g/cm), or $m_{A,SELF\ AVG}$ ($\mathrm{g/cm^2}$), respectively. The corresponding result for the total isotope mass in a piece of equipment is

$$m\ (\mathrm{g}) = m_{P,SELF\ AVG} \quad , \tag{53}$$

$$m\ (\mathrm{g}) = (L_{TOT}) \bullet m_{L,SELF\ AVG} \quad , \tag{54}$$

or

$$m\ (\mathrm{g}) = (A_{TOT}) \bullet m_{A,SELF\ AVG} \quad , \tag{55}$$

for measurement of a point, line, or area deposit, respectively. To obtain the total mass of the element from the mass of the isotope, divide Eqs. (53–55) by the isotope fraction f_I. The contribution of counting statistics to the measurement uncertainty diminishes considerably in this averaging process.[3] The use of very short count times at many locations on a given piece of equipment enables the result obtained in Eq. (53), (54), or (55) to be more representative of the equipment, despite a nonuniform deposit thickness. There is no loss of precision, statistically, in this approach. However, the number of measurements increases greatly and the overhead in cost could be prohibitive without automation of much of the measurement process as well as the analysis.

VII. SENSITIVITY OF THE SPECIFIC MASS TO THE UNCERTAINTY IN *w*

A. Introduction

The choice of a width parameter *w* is the first step in the process of correcting for the negative bias caused by the finite dimensions of a holdup deposit or self-attenuation of its gamma rays. These corrections are key to eliminating the negative bias in gamma-ray holdup measurements. Uncertain knowledge of *w* should not deter the use of these corrections. If they are carried out with the best information available on *w*, the bias is eliminated on average because the result for holdup is sometimes low and sometimes high rather than always low.

Errors in the experimental width parameter *w* chosen by the user will introduce systematic effects in the specific mass corrected for finite source dimensions and subsequently for self-attenuation. However, *w* is the same parameter used for both corrections, and the sign of the systematic effect is opposite for the two corrections. For very thick deposits not typical of holdup but found occasionally in process equipment, the self-attenuation effect dominates the corrections, and the systematic effect of the uncertainty in *w* is effectively determined by this correction alone. For thinner deposits more typical of holdup, the systematic effect of the uncertainty in *w* is affected by both corrections, tending to reduce the overall error incurred by errors in the knowledge of *w*.

This section looks at the magnitude of the correction for finite-source and self-attenuation effects (individually and combined) as a function of deposit thickness for the collimator and measurement geometry illustrated (measurement distance *r* of 40 cm, and a collimator diameter and depth of 2.54 cm) in Figs. 1 and 9. It demonstrates the inherent bias that results when the corrections are ignored. It also illustrates self-consistent limitation in the total error in the measured holdup for individual holdup deposits despite uncertain knowledge of the common parameter *w* used to describe the width of holdup deposits for both types of corrections. For the examples calculated below, it is assumed that *w* is 10 cm, which is both a common duct dimension and significant fraction of the dimension of the field of view at the 40-cm (*r* and r_0) measurement distance. If the concentric circles in Figs. 7 and 8 are spaced by 5 cm, these two sketches match Figs. 2 and 9 and represent this sample geometry for the line and point source, respectively. The example deposit chosen is uranium (f_I = 93%) for which the self-attenuation effects on the 186-keV gamma ray of ^{235}U are larger than those for the 414-keV gamma ray of ^{239}Pu in plutonium deposits of the same thickness.

The units in Figs. 11-20 are those of specific mass for point, line and area deposits (g, g/cm, and g/cm^2, respectively). However, specific mass has been symbolized in terms of areal density ρx for point, line, and area deposits (aρx, wρx, and ρx, respectively, instead of m_P, m_L, and m_A) to point out the relationship to the results for true vs measured areal density plotted in Fig. 10.

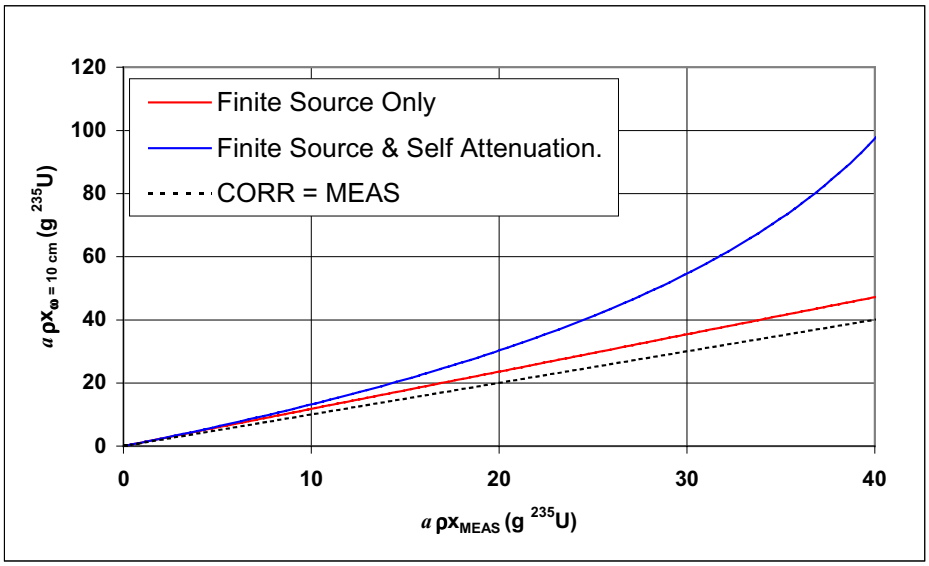

Fig. 11. Corrected vs measured specific mass is plotted for the finite point deposit. The deposit width parameter w of 10 cm is the diameter of the point deposit and corresponds to an area parameter a of 79 cm^2 for the point deposit. The dashed line drawn for reference passes through the origin with a slope of 1. The middle (red) line is the specific mass of the finite point source corrected for the finite-source effect only. The top (blue) line includes the additional correction for self-attenuation.

B. Point Deposit

Figure 11 shows the corrected vs measured specific mass for the finite point deposit. The deposit width parameter w of 10 cm corresponds to an area parameter a of 79 cm^2 (Eq. 23) for the point deposit. The dashed line drawn for reference passes through the origin with a slope of 1 (effectively plotting an uncorrected result) to guide the eye in visualizing the magnitude of the corrections. The center (red) line, determined from Eqs. (14) and (22), is the specific mass of the finite point deposit corrected for the finite source dimension w only. The top (blue) line includes the additional correction for self-attenuation, Eqs. (38), (47), and (50). It is apparent that the self-attenuation correction dominates for the thickest deposits. Figure 12 shows the percent difference between the corrected and measured specific mass vs the measured value of the point deposit. The relative finite-source correction (bottom line) is constant, and the relative self-attenuation correction (top line) increases nonlinearly with areal density. Below ~10 g ^{235}U (~0.1 g/cm^2), the finite-source effect is actually larger than the self-attenuation effect. For all measured thicknesses of the point deposit, the measured result is biased low before the corrections are applied.

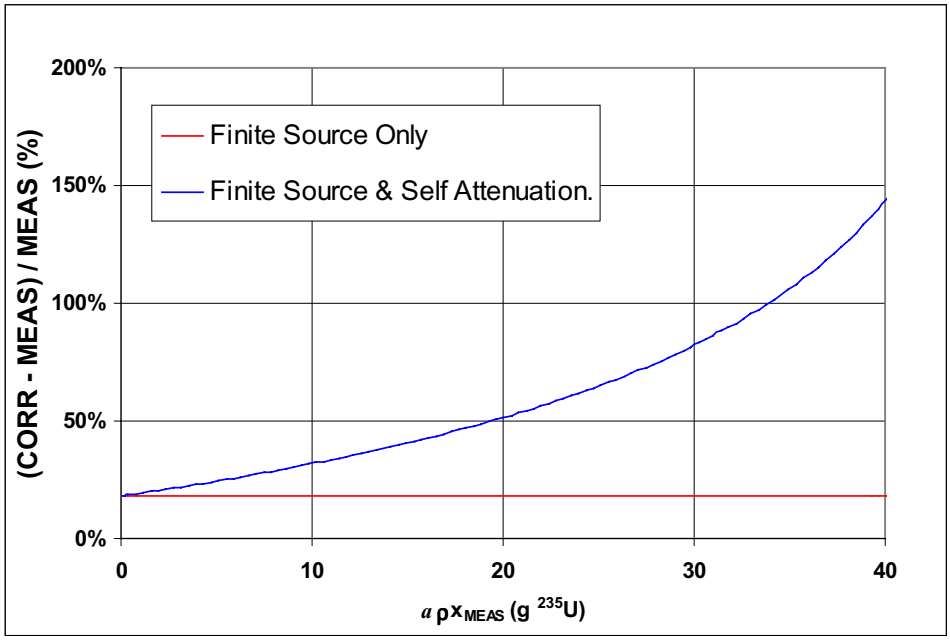

Fig. 12. Percent difference between the corrected and measured specific mass vs the measured value is plotted for a point deposit. The deposit width parameter w of 10 cm corresponds to an area parameter a of 79 cm^2 for the point source. The relative finite-source correction (bottom line in red) is constant and the relative self-attenuation correction (top line in blue) increases nonlinearly with areal density. Below ~10 g ^{235}U (~0.1 g/cm^2, in this case), the finite-source effect exceeds the self-attenuation effect.

Figure 13 shows data analogous to the blue curve in Fig. 11. It plots the corrected (for finite-source and self-attenuation effects both) vs the measured specific mass, but the correction is performed for three values of the deposit width parameter. If 10 cm is the true deposit width, then 7.5 and 15 cm represent 33% under- and 33% over-estimates of w, respectively. Above 20 g ^{235}U (~0.2 g/cm^2), which is an unusually thick deposit compared to most holdup, the curves diverge significantly. Here, where self-attenuation dominates the correction, a 33% over-estimate of w (w = 15 cm) gives a result that is increasingly low with increasing thickness. Similarly, a 33% under-estimate of w (w = 7.5 cm) gives a result that is increasingly high with increasing thickness. However, the behavior below 20 g ^{235}U (~0.2 g/cm^2) is similar for the three values of w.

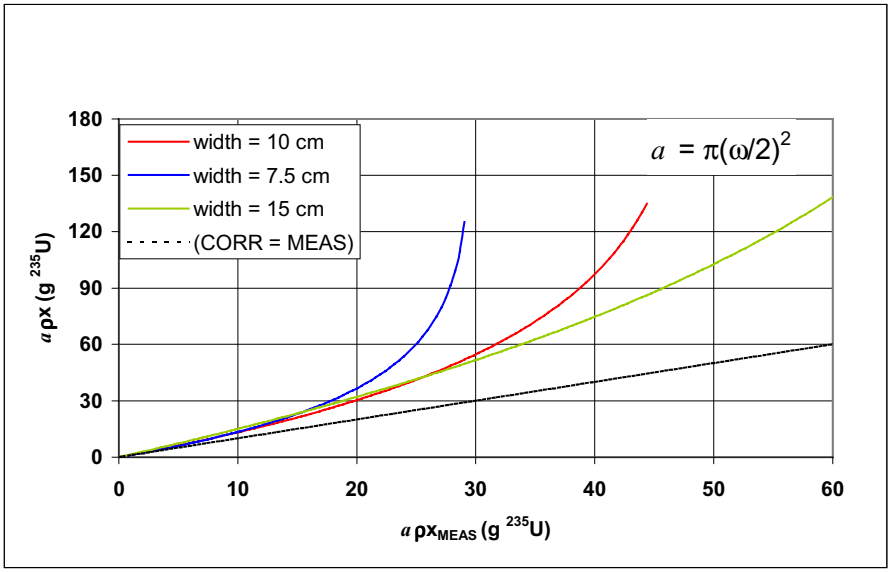

Fig. 13. The corrected (for both finite-source and self-attenuation effects) vs the measured specific mass, is plotted for three values of the point deposit width parameter. The true deposit width parameter w of 10 cm (red – middle curve) corresponds to an area parameter a of 79 cm^2 for the point source. The width parameters of 7.5 (blue – middle curve) and 15 (green – bottom curve) cm under- and over-estimate (respectively) w by 33%.

Figure 14 magnifies the detail of this behavior up to 20 g ^{235}U (~0.2 g/cm^2, a realistic upper limit of areal density for most holdup deposits) with a plot of the percent difference between the corrected and true (w = 10 cm) specific mass vs the measured value. The dashed horizontal line at 0% difference is the plot for the true (w = 10 cm) result. The red (bottom) line is the uncorrected (measured) result. It is always biased negatively and the bias increases with deposit thickness. The blue (middle) line, corresponding to a 33% under-estimate of w (w = 7.5 cm) starts out negatively biased (where the finite-source effect dominates) and gradually becomes positively biased (where the self-attenuation effect dominates), but the bias shrinks with increasing thickness (because of the compensating effect of the two corrections) and is always less than that of the uncorrected result. The green (top) line, corresponding to a 33% over-estimate of w (w = 15 cm) starts out with a positive bias (where the finite-source effect dominates) that shrinks with increasing thickness as the self-attenuation effect grows (because of the compensating effect of the two corrections). Except for the very thinnest deposits where the bias represents a very small quantity, the overall bias is always smaller than the bias in the uncorrected result for the point deposit.

Figure 14 demonstrates that in the thickness range of most holdup point deposits, over- and under-estimates of w cause errors in the corrected result that (1) are respectively opposite in sign, (2) decrease with increasing thickness, and (3) are smaller than the always negative and monotonically increasing (with deposit thickness) bias in the uncorrected result. Figure 14 presents a strong argument in favor of performing corrections for both finite-source and self-attenuation effects for all point deposits of holdup.

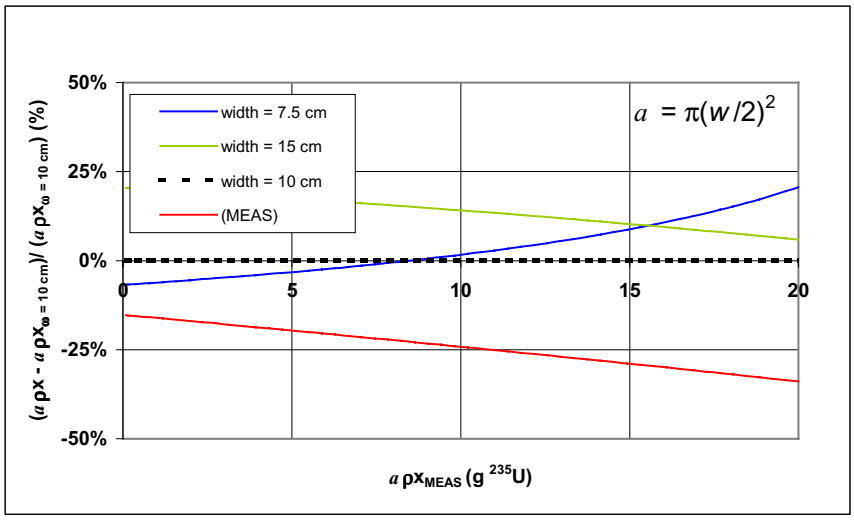

Fig. 14. Percent difference between the corrected and true (w = 10 cm) specific mass of a point deposit vs the measured value is plotted in a realistic mass range for holdup. The true deposit width parameter w of 10 cm corresponds to an area parameter a of 79 cm^2 for the point source. The dashed horizontal line at 0% difference is the plot for the true (w = 10 cm) result. The red (bottom) line is the uncorrected (measured) result. The blue line (middle, curved upward) corresponds to a 33% under-estimate of w (w = 7.5 cm). The green (top) line corresponds to a 33% over-estimate of w (w = 15 cm).

C. Line Deposit

Figure 15 shows the corrected vs measured specific mass for the finite line source. The deposit width parameter *w* of 10 cm corresponds to the width of the line deposit. The dashed line drawn for reference passes through the origin with a slope of 1 (effectively plotting an uncorrected result) to guide the eye in visualizing the magnitude of the corrections. The red line, determined from Eqs. (15) and (21), is the specific mass of the finite line deposit corrected for the finite source dimension *w* only. The blue line includes the additional correction for self-attenuation, Eqs. (39), (48), and (51). It is apparent that the self-attenuation correction dominates for the thickest deposits. Figure 16 shows the percent difference between the corrected and measured specific mass vs the measured value of the line deposit. The relative finite-source correction is constant and the relative self-attenuation correction increases nonlinearly with areal density. Below ~1 g ^{235}U (~0.1 g/cm^2, in this case), the finite-source effect is actually larger than the self-attenuation effect. For all measured thicknesses of the line deposit, the measured result is biased low before the corrections are applied.

Figure 17 shows data analogous to the blue curve in Fig. 15. It plots the corrected (for finite-source and self-attenuation effects) vs the measured specific mass, but the correction is performed for three values of the deposit width parameter. If 10 cm is the true deposit width, then 7.5 and 15 cm represent 33% under- and 33% over-estimates of *w*, respectively. Above 2 g ^{235}U/cm (~0.2 g/cm^2), which is an unusually thick line deposit compared to most holdup, the curves diverge significantly. Here, where self-attenuation dominates the correction, a 33% over-estimate of *w* (*w* = 15 cm) gives a result that is increasingly low with increasing thickness. Similarly, a 33% under-estimate of *w* (*w* =

7.5 cm) gives a result that is increasingly high with increasing thickness. However, the behavior below 2 g ^{235}U/cm (~0.2 g/cm^2) is similar for the three values of *w*.

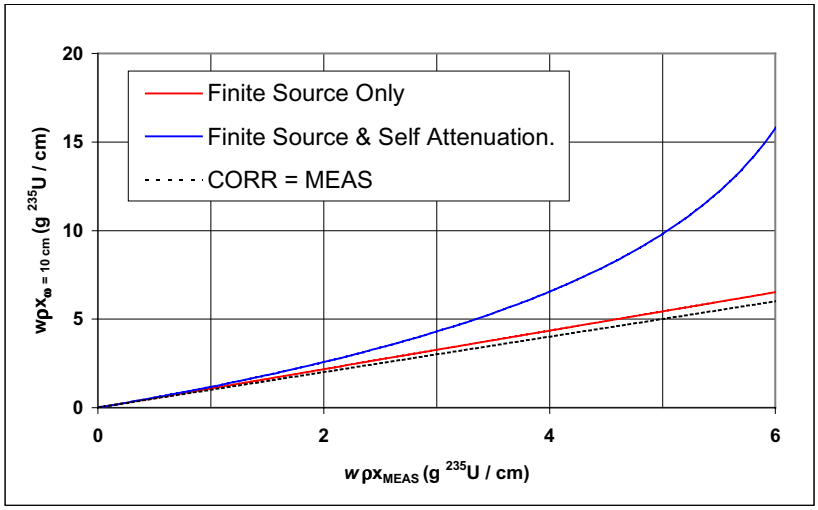

Fig. 15. Corrected vs measured specific mass for the finite line source. The deposit width parameter w of 10 cm is the width of the line deposit. The dashed line drawn for reference passes through the origin with a slope of 1. The red (middle) line is the specific mass of the finite line deposit corrected for the finite-source effect only. The blue (top) line includes the additional correction for self-attenuation.

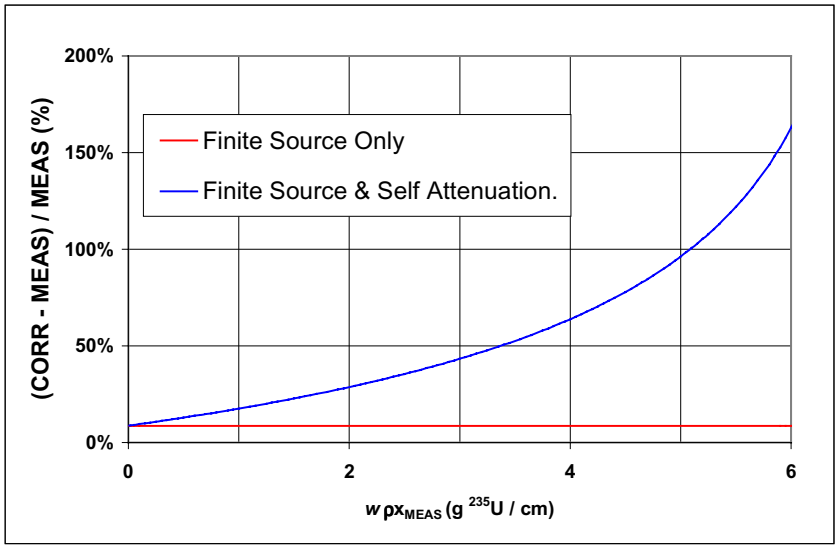

Fig. 16. Percent difference between the corrected and measured specific mass is plotted vs the measured value for a line deposit. The deposit width parameter w of 10 cm corresponds to the width parameter for the line deposit. The relative finite-source correction (horizontal red line) is constant, and the relative self-attenuation correction (curved blue line) increases nonlinearly with areal density. Below ~1 g ^{235}U/cm (~0.1 g/cm^2, in this case), the finite-source effect exceeds the self-attenuation effect.

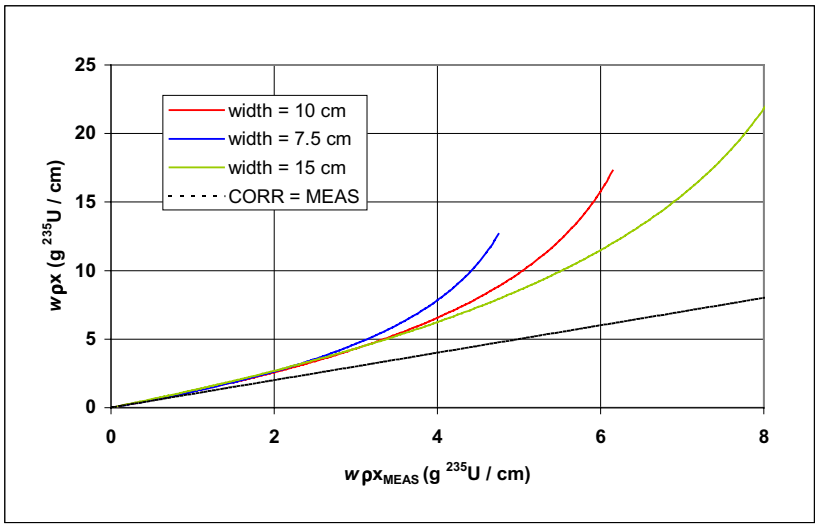

Fig. 17. The corrected (for both finite-source and self-attenuation effects) vs the measured specific mass is plotted for three values of the line deposit width parameter. The true deposit width parameter w of 10 cm (red) is the width of the line source. The width parameters of 7.5 (blue) and 15 (green) cm under- and over-estimate (respectively) w by 33%.

Figure 18 magnifies the detail of this behavior for a line deposit with up to 4 g ^{235}U/cm (~0.4 g/cm^2) in a plot of the percent difference between the corrected and true (w = 10 cm) specific mass vs the measured value. The dashed horizontal line at 0% difference is the plot for the true (w = 10 cm) result. The red line is the uncorrected (measured) result. It is always biased negatively and the bias increases with deposit thickness. The blue line, corresponding to a 33% under-estimate of w (w = 7.5 cm), starts out negatively biased (where the finite-source effect dominates). It gradually becomes positively biased (where the self-attenuation effect dominates), but the bias shrinks with increasing thickness (because of the compensating effect of the two corrections) and is always less than that of the uncorrected result. The green line, corresponding to a 33% over-estimate of w (w = 15 cm), starts out positively biased (where the finite-source effect dominates) and shrinks with increasing thickness as the self-attenuation effect grows (because of the compensating effect of the two corrections). Except for the very thinnest deposits where the bias represents a very small quantity, the overall bias is always smaller than the bias in the uncorrected result for the line deposit.

Figure 18 demonstrates that in the thickness range of most holdup line deposits, over- and under-estimates of w cause errors in the corrected result that (1) are respectively opposite in sign, (2) decrease with increasing thickness, and (3) are smaller than the always negative and monotonically increasing (with deposit thickness) bias in the uncorrected result. Figure 18 presents a strong argument in favor of performing corrections for both finite-source and self-attenuation effects for all line deposits of holdup.

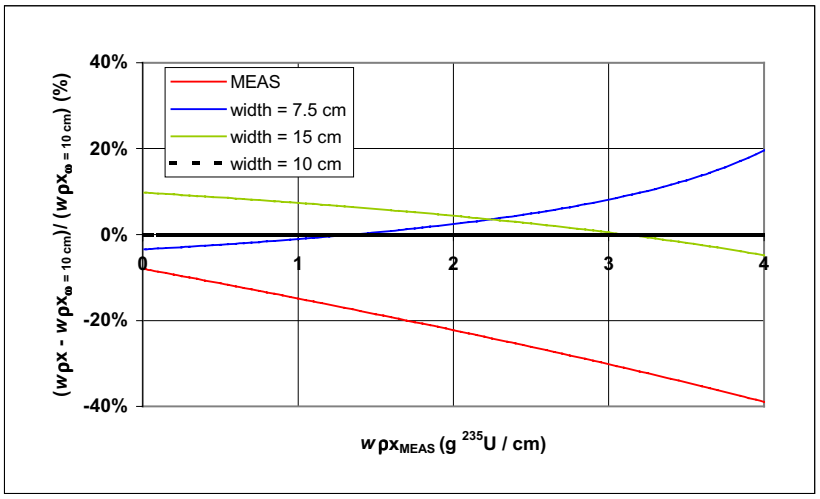

Fig. 18. Percent difference between the corrected and true specific mass of a line deposit vs the measured value. The true deposit width parameter w of 10 cm is the width of the line deposit. The dashed horizontal line at 0% difference is the plot for the true (w = 10 cm) result. The red (bottom) line is the uncorrected (measured) result. The blue (middle, curving upward) line, corresponds to a 33% under-estimate of w (w = 7.5 cm). The green (top, curving downward) line corresponds to a 33% over-estimate of w (w = 15 cm).

D. Area Deposit

The width parameter does not apply to an area deposit because a finite area deposit fills the detector field of view. Figure 19 shows the corrected vs measured specific mass for the area deposit. The dashed line drawn for reference passes through the origin with a slope of 1 (effectively plotting an uncorrected result) to guide the eye in visualizing the magnitude of the correction. Because the finite width exceeds the detector field of view, there is no correction for the finite dimension of an area source. The blue line includes the correction for self-attenuation only, Eqs. (40), (49), and (52).

Figure 20 shows the percent difference between the corrected and measured specific mass vs the measured value of the area deposit. The areal density of most holdup deposits is less than 0.2 g/cm^2. However, for all measured thicknesses of the area deposit, the measured result is biased low before corrections for self-attenuation are applied.

Figures 19 and 20 demonstrate that in the entire thickness range of holdup area deposits, the correction for self-attenuation increases with increasing deposit thickness. The correction for self-attenuation does not require knowledge of an empirical width parameter. It uses only the measured value of the specific mass, which is the areal density in the case of an area deposit. This presents a strong argument in favor of performing corrections for self-attenuation effects for all area deposits of holdup.

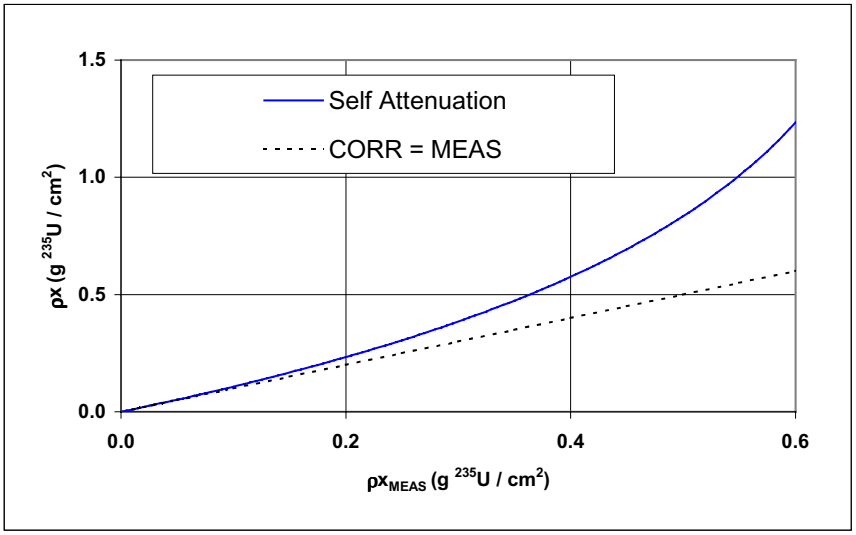

Fig. 19. Corrected vs measured specific mass for the area source. The width of an area deposit exceeds the width of the field of view of the detector. Therefore, there is no correction for the dimension of the finite source. The dashed line drawn for reference passes through the origin with a slope of 1. The solid blue line includes the correction for self-attenuation.

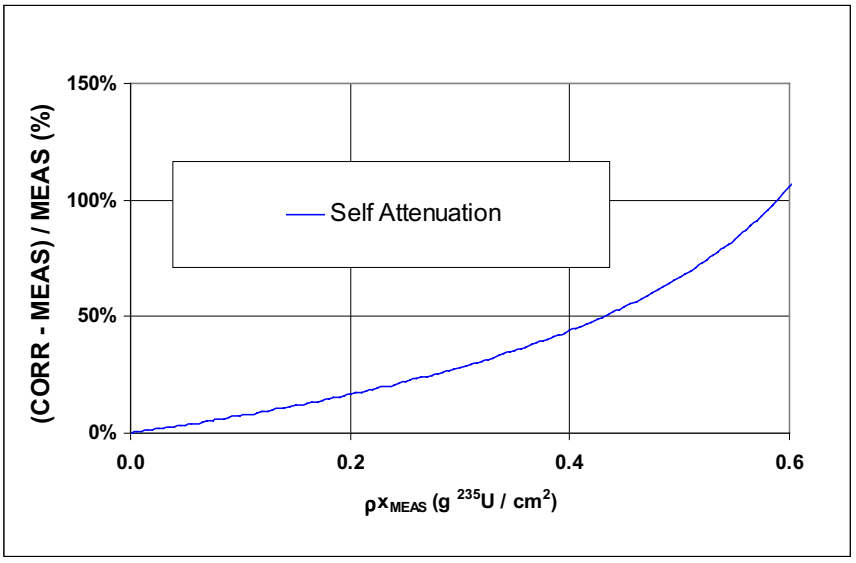

Fig. 20. Percent difference between the corrected and measured specific mass vs the measured value for an area deposit. The width of an area deposit exceeds the width of the field of view of the detector. Therefore, there is no correction for the finite dimension of the deposit. The relative self-attenuation correction (blue) increases nonlinearly with areal density.

VIII. AUTOMATED IMPLEMENTATION OF CORRECTION ALGORITHMS

The HMS3[11-12] holdup measurement program allows a user to perform hundreds of measurements of holdup deposits, analyze their results, and report the total holdup within a matter of hours. It is designed to enable the routine and plant-wide measurement of holdup, which may require thousands of discrete measurements during each monthly or bimonthly inventory period. The execution is streamlined by scanning the barcodes at the individual measurement locations and by using a database that contains information on the measurement location and equipment dimension for each bar-coded position. Without automation provided by the equivalent of the HMS3 software, it is not possible to execute the large-scale campaigns that are required for inventory in a large facility.

Two Visual Basic (VB) subroutines have been written to operate with (and eventually within) the HMS3 software to perform corrections for finite source dimensions and self-attenuation effects in holdup measurements based on the GGH formalism. The correction algorithms are those derived in Sections IV and V above. The subroutines currently address holdup of ^{235}U (based on measurements of the 186-keV gamma ray) and ^{239}Pu (based on measurements of the 414-keV gamma ray). However, they can be modified readily for other isotopes. The algorithms are independent of the type of gamma-ray detector (NaI, CdZnTe, HPGe, etc.) used to perform the measurements.

The input for the two new subroutines is provided by the current HMS3 analysis. This is the specific isotope mass of a point, line, or area deposit: $m_{P,EQ}$ (g) from Eq. (11), $m_{L,EQ}$ (g/cm) from Eq. (12), and $m_{A,EQ}$ (g/cm^2) from Eq. (13), respectively. These measured quantities are corrected by the existing HMS3 software for the effects of room background and equipment attenuation according to the procedures described in Sections II and III above. All parameters that are required to automate Sections II and III are currently stored in the HMS3 calibration files or the process equipment database.

Figure 21 is the user-interface screen for the stand-alone VB program, *Finite v. 1.0*. The screen displays the finite-source correction factor $CF_{FIN,L}$ or $CF_{FIN,P}$ of the specific mass of a point or line deposit, respectively, as defined in Eqs. (21) or (22). This correction factor is evaluated by the software based on a Gaussian form for the radial response. The user-interface screen accepts input of the Gaussian parameters for the radial response for each detector by one of two methods. The first is manual entry of the FWHM of the normalized (to 1 at the peak) radial response. The FWHM is used in the VB code to determine the "a" and "b" parameters of the normalized Gaussian:

$$G(x) = a \bullet \exp(-bx^2)$$

where

$$a = 1$$

and

$$b = 0.5(2.354/FWHM)^2 \quad ,$$

consistent with Eq. (18). Alternatively, as illustrated in Fig. 21, the "a" and "b" parameters from a Gaussian fit to the radial response may be input directly on the screen.

The user may store default values for “a” and “b” in an initialization file of the VB program to simplify the startup process.

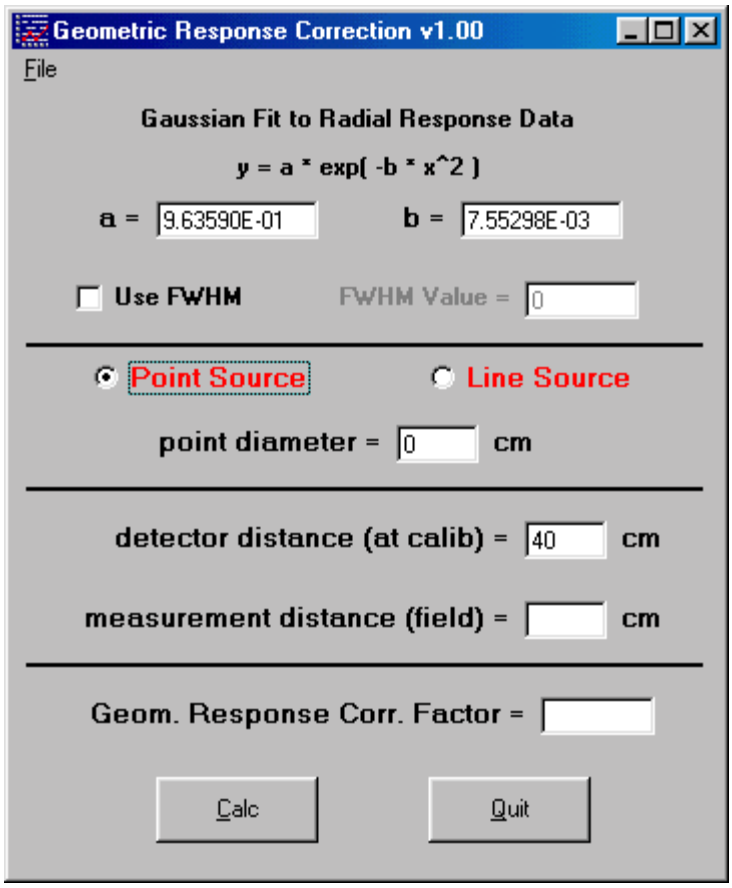

Fig. 21. User-interface screen for the stand-alone VB program, Finite v. 1.0, which determines the finite-source correction factor $CF_{FIN,P}$ or $CF_{FIN,L}$ of the specific mass of a point or line deposit, respectively. The “a” and “b” parameters for the Gaussian fit to the radial response of the detector have been entered directly on the screen displayed. This sample screen is for an infinitely small point source measured by a detector whose calibration distance r_0 was 40 cm.

The screen is also used to choose the deposit geometry (point or line) and the finite source dimension w (point diameter or line width, respectively). Finally, it requires input of the calibration distance r_0 (for which the Gaussian form is valid) and the measurement distance r. The user may also store a default (startup) value for r_0 in the initialization file of the VB program.

Figure 22 is the user-interface screen for the stand-alone VB program, *SelfAttn v. 1.0*. The screen displays the self-attenuation-corrected specific isotope mass ($m_{P,SELF}$, $m_{L,SELF}$, or $m_{A,SELF}$, respectively) of a point, line, or area deposit, as defined in Eqs. (50-52). Therefore, the required input includes the finite-source-corrected specific mass $m_{P,FIN}$, $m_{L,FIN}$, or $m_{A,FIN}$ of the isotope defined by Eqs. (14), (15), or (16) for a point, line or area source, respectively. Because the uncertainty in the self-attenuation-corrected

specific mass is a nonlinear function of the uncertainty in the finite-source-corrected specific mass, the uncertainty in $m_{P,FIN}$, $m_{L,FIN}$, or $m_{A,FIN}$ is also required input. The uncertainty in $m_{P,SELF}$, $m_{L,SELF}$, or $m_{A,SELF}$ is displayed for each calculation.

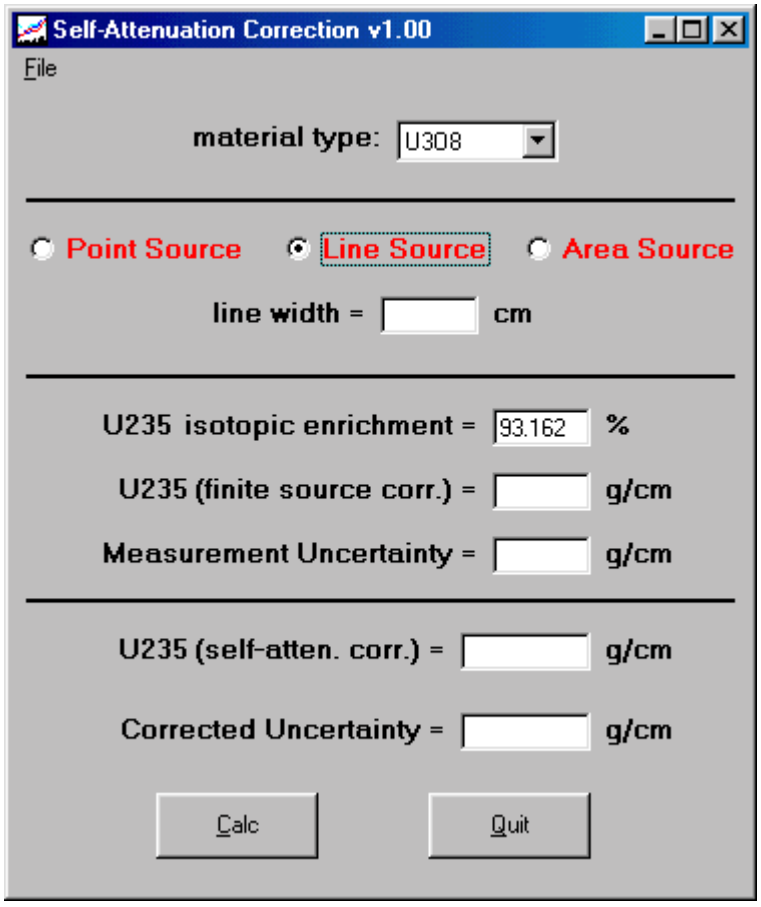

Fig. 22. User-interface screen for input to the stand-alone VB program SelfAttn v. 1.0 that determines the self-attenuation-corrected specific isotope mass (and its uncertainty) for a point, line or area deposit. This sample screen is set up for a line deposit of ^{235}U as U_3O_8 with an isotopic enrichment of 93.162%. The finite-source-corrected specific mass of ^{235}U ("finite source corr.") and its uncertainty ("Measurement Uncertainty") are required input. For the line and also for a point deposit, the finite-source dimension w ("line width" or "point diameter", respectively) is also required.

The corrected result and its uncertainty is determined, as described in Section V, after converting the specific mass of the isotope to that of the actinide and evaluating the corresponding areal density of the deposit. Equations (28–31) and f_I (the "isotopic enrichment") are used for the conversion to actinide values. Equations (32–34) and *w* (the same deposit width parameter used as input to *Finite v. 1.0*) are used to convert specific mass to areal density.

Two limiting conditions are tested in the VB program for the self-attenuation correction. One imposed on the uncorrected areal density, as defined by Eq. (27), where K is three, addresses the problem of infinitely thick deposits. If Eq. (27) is satisfied, the

message box illustrated in Fig 23(a) appears, and the correction is not performed. The second condition imposed on the corrected areal density is a limitation on its relative error. The relative error in the corrected specific mass of the deposit increases nonlinearly with increasing areal density of the deposit, as described in Eqs. (41–43). For a point, line or area deposit, respectively, if Eq. (44), (45), or (46) is satisfied (where F is 0.5), the relative error exceeds 50%, the message box illustrated in Fig 23(b) appears, and the correction is not performed.

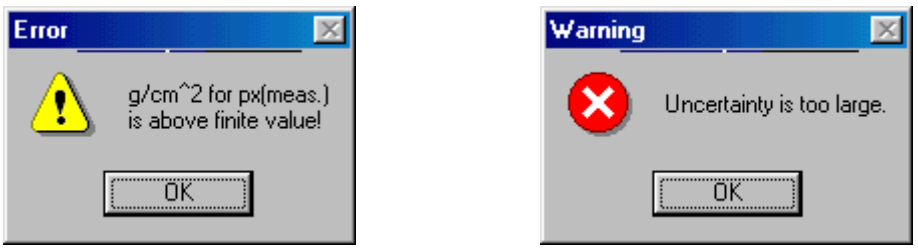

(a) **(b)**

Fig. 23. Message boxes that appear during the execution of SelfAttn v. 1.0 if (a) the uncorrected areal density of the deposit (statistically) approaches a thickness that is infinite relative to the assay gamma ray, and (b) the relative uncertainty in the areal density of the corrected areal deposit exceeds 50%. For either circumstance, the calculation of the self-attenuation-corrected isotope specific mass is not completed, and the corrected result is not displayed.

For implementation of the subroutines in the next generation of the HMS3 software, only one additional parameter is required in the database for each bar-coded measurement position. The new parameter will be stored in a location that was reserved for it when the database was created, so that the database itself remains unchanged. The new quantity is the empirical width parameter, w, of the holdup deposit (the diameter of a point deposit or the width of a line deposit) that is part of the operator's knowledge of the process and its holdup. All other requirements for execution of the two subroutines are either parameters that are already stored in the database for the detector or measurement location, or are results of the analysis of the measurement data. The formality of the implementation of the corrections for finite source dimensions and self-attenuation effects under GGH enables the automation of these corrections.

IX. REDUCTION OF BIAS FROM INTERFERENCE EFFECTS

The performance of a gamma-ray detector can contribute to bias in the assay of holdup deposits of uranium or plutonium. Discrete interferences between the assay gamma ray and other gamma rays that arise from room background or the holdup deposit itself can add unwanted counts to the assay peak or the background region. This can cause the quantitative result to be biased high or low, respectively. The Compton edge from a high-energy gamma ray can be situated between the peak and background analysis regions for the assay gamma ray, causing the assay to be biased high, typically. Such problems are documented for low-resolution gamma-ray measurements of uranium[17] and plutonium,[18] respectively, in which NaI(Tl) detectors are used.

Detectors with improved performance (energy resolution and peak shape) will contribute to reductions in bias from interference effects in spectroscopic assays. The use of high-resolution HPGe detectors is generally not possible for routine measurements of holdup plant-wide. The shielded detectors are far too heavy and large to be practical in these applications. The size/weight of the HPGe detectors is limited by the requirements that cooling to cryogenic temperatures imposes on the detector design. For many years, alternative solid-state detectors that operate at room temperature (CdTe, HgI_2, etc.) have been anticipated as replacements for NaI(Tl) scintillator detectors in applications to portable gamma-ray spectroscopy for holdup measurements. Until recently, such detectors with crystals of sufficient size to have the sensitivity required for holdup measurements have not been produced. Recent commercial progress with the new coplanar-grid CdZnTe detectors[19–22] indicates that a transition in the technology for portable gamma-ray measurements of holdup will take place.

The energy resolution (FWHM) and the peak shape (FWTM / FWHM) are used to compare the performance of compact NaI(Tl) detectors designed for portable gamma-ray spectroscopy of holdup with the performance of the new, large, coplanar-grid CdZnTe detectors. The sample data in Table II indicates that as of 1998, the performance characteristics of the coplanar-grid CdZnTe detector included comparable peak shapes and an energy resolution for gamma rays in the range of 100–600 keV, two to three times better than that of NaI(Tl) detectors. While the detection efficiency is two-and-a-half to three times lower, the sensitivity is equivalent in this energy range because of the improved spectroscopic signal-to-background ratio that better resolution provides. Adding to the benefits for holdup measurements, the new solid-state detectors are more compact, reliable, and stable than scintillators. However, the spectroscopic advantage of the improved energy resolution will eliminate bias that is incurred in many types of portable measurements, holdup being an important one of these, that are subject to spectroscopic interferences from variable backgrounds.

Table II.

NaI(Tl) and Coplanar-Grid CdZnTe Detectors: Comparison Data

Compact Room-Temperature Gamma-ray Detector		Compact NaI(Tl) Detector	Replacement: CPG CdZnTe	
			July 1997	September 1998
122 keV*	% FWHM	14.5	16.9	6.2
	FWTM/FWHM	1.9	1.9	1.9
662 keV**	% FWHM	8.0	3.6	2.8
	FWTM/FWHM	1.8	2.1	2.2
% Relative Efficiency	122 keV	100	40	40
(CdZnTe / NaI)	662 keV	100	30	30
Crystal shape		Cylindrical	Rectangular	Rectangular
Crystal cross-sectional area, cm^2		5.1	2.3	2.3
Crystal depth, cm		5.1	1.5	1.5

* benchmark gamma ray for assay of ^{235}U

** benchmark gamma ray for assay of ^{239}Pu

Figure 24 is an example of the spectroscopic advantage provided by the large coplanar-grid CdZnTe detector in measurements of enriched uranium with interfering gamma rays from the ^{232}U-^{232}Th decay chain, whose signatures appear in recycled material. The measurements represented by the overlaid HPGe, coplanar-grid CdZnTe and NaI(Tl) spectra in Fig. 24 were made simultaneously and *in situ* in a uranium facility.[17] A high-energy gamma–ray continuum background in this plant environment destroys the sensitivity that might be achieved in a laboratory environment, and interferences from recycle decay products contribute to bias in the assay based on the 186-keV gamma ray in this facility. A major gamma ray at 238 keV is produced at the end of the ^{232}U-^{232}Th decay chain. This gamma ray is not resolved from the 186-keV gamma ray of ^{235}U in the NaI(Tl), but does not interfere with the 186-keV analysis in either the HPGe or the coplanar-grid CdZnTe gamma-ray spectra. The holdup measurements in progress in this facility use the coplanar-grid CdZnTe detectors.

The effects of gamma ray peaks from ^{241}Pu-^{237}U (332 keV), ^{241}Am (323-335 keV, 662 keV), and ^{237}Np-^{233}Pa contribute to bias in the NaI(Tl) holdup assay of ^{239}Pu at 414 keV.[9,18,23] Many of these effects are readily addressed with the improved performance of the coplanar-grid CdZnTe detector. Further improvements that will be realized through response-function analysis of the CdZnTe gamma-ray spectra[19] are required to address the worst of these interference effects caused by the ^{237}Np-^{233}Pa decay. Because of the complexity of these gamma-ray spectra, an analysis of this type to resolve discrete interferences is not possible with the low resolution of NaI(Tl) detectors.

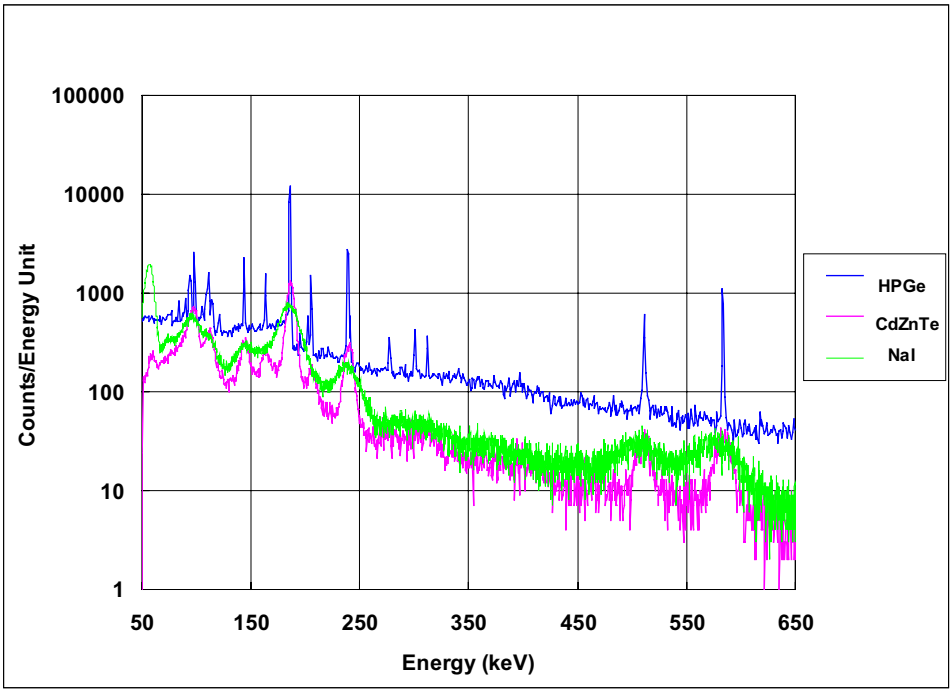

Fig. 24. Gamma-ray spectra obtained with three shielded, portable detectors: HPGe, coplanar-grid CdZnTe, and NaI(Tl). The gains are approximately matched for the three spectra. The measurements were performed in a uranium facility in which high-energy γ rays penetrate the shielding on the detectors to increase the continuum under the 186-keV peak of ^{235}U. The gamma ray at 238 keV from the ^{232}U-^{232}Th decay chain appears with variable intensity relative to the 186-keV gamma ray throughout the facility. This is an interference in the NaI(Tl) spectrum, but it is well resolved with HPGe and CdZnTe.

X. SUMMARY

A generally useful approach to the quantitative measurements of holdup invokes simple, geometric models (point, line, and area) to describe the holdup deposits. The result is that simple calibration procedures and assay algorithms apply to most deposits, despite the unique geometry of each. Until recently, only the effects of room background and equipment attenuation have been used to adjust the reduced spectral data for effects that would otherwise bias the quantitative GGH results. Because of the simplicity and generality of this GGH approach, rapid portable assays of extensive holdup can be performed plant-wide with the aid of automation of the measurements, reduction, and analysis of spectral data and computation of plant-wide holdup.

Two other major sources of bias, both of which cause the assay results to be low if ignored, are now addressed in a new analysis protocol under the GGH formalism. One effect arises from the finite dimensions of point and line deposits, which the GGH models assume to be infinitely narrow compared to the detector's relatively wide field of view. The other effect is caused by the self-attenuation of gamma rays by the deposit. Using the new protocol under GGH, knowledge of the width of a point or a line deposit is sufficient to perform both corrections self-consistently. Furthermore, the error that arises in the finite-source correction from uncertain knowledge of the width of a point or a line deposit is partially cancelled by an error of the opposite sign in the corresponding self-attenuation correction in the thickness range of most holdup deposits. It is compelling, therefore, to

apply both corrections self-consistently. For area deposits, only the self-attenuation correction applies. It is independent of an additional parameter and is determined directly from the uncorrected holdup result.

Like the GGH approach, implementation of the finite-source and self-attenuation corrections is simple and applies generally to all cases. Therefore, the new corrections are easily automated too.

Although the corrections for the effects of finite source dimensions and self-attenuation of gamma rays are of the order of a few percent for most holdup deposits, they should not be ignored. The resulting negative bias arises in every measurement, and a small percentage bias in the plant-wide holdup is a large absolute quantity.

There is a tendency for the relative finite-source effects to be larger for holdup measurements of ^{239}Pu and for the relative self-attenuation effects to be larger for holdup measurements of ^{235}U. Each tendency is a result of the gamma-ray assay energy for each isotope. The higher energy gamma ray used to measure ^{239}Pu penetrates the detector shield readily, causing users to perform measurements closer to the deposits. A relative enlargement of the finite source dimension is the result of the reduction in the detector's field of view at the smaller measurement distance. The lower energy gamma ray used to measure ^{235}U is more affected by self-attenuation. However, the detector shielding is quite effective at eliminating room background, causing users to perform measurements at greater distance from the deposits. The result is a reduction in the relative finite source dimension.

A final major source of bias in holdup measurements arises from the relatively poor resolution of the portable, compact scintillator detectors that are used for gamma-ray spectroscopy in these applications. Effects of interfering gamma rays from complex spectra can contribute to a positive or negative bias in the holdup result obtained from measurements with scintillators. The portability of a room-temperature detector cannot be sacrificed in holdup applications. Therefore, recent progress in the manufacturing of large, room-temperature, solid-state gamma-ray detectors that perform better than scintillators is a welcome advance in technology for improved accuracy in holdup measurements.

REFERENCES

1. "In-Situ Assay of Enriched Uranium Residual Holdup," NRC Regulatory Guide 5.37, Rev. 1, United States Nuclear Regulatory Commission (October 1983), Washington D.C.

2. "In-Situ Assay of Plutonium Residual Holdup," NRC Regulatory Guide 5.37, Rev. 1, United States Nuclear Regulatory Commission (February 1984), Washington D.C.

3. "Nondestructive Assay of Special Nuclear Materials Holdup," Los Alamos National Laboratory training manual LA-UR-99-2597 (August 1999 or earlier versions, beginning in February 1991).

4. P. A. Russo, H. A. Smith, J. K. Sprinkle, Jr., C. W. Bjork, G. A. Sheppard, and S. E. Smith, "Evaluation of an Integrated Holdup Measurement System Using the GGH

Formalism with the M^3CA," published in the *Proceedings of the Fifth International Conference on Facility Operation – Safeguards Interface*. LaGrange Park, IL: American Nuclear Society (1996), pp. 239-248.

5. J. K. Sprinkle, Jr., R. Cole, M. L. Collins, S.-T. Hsue, P. A. Russo, R. Siebelist, H. A. Smith, Jr., R. N. Ceo and S. E. Smith, "Low-Resolution Gamma-Ray Measurements of Process Holdup," Los Alamos National Laboratory report LA-UR-96-3482 (Presented at the *Third Topical Meeting on Industrial Radiation and Radioisotope Measurements and Applications;* Raleigh, North Carolina; October 1996).

6. G. A. Sheppard, P. A. Russo, M. C. Miller, T. R. Wenz, E. C. Piquette, F. X. Haas, J. B. Glick, and A. G. Garrett, "Models for Gamma-Ray Holdup Measurement at Duct Contact," *Nucl. Mater. Manage.* **XXI** (Proc. Issue) 68–73 (1991).

7. J. B. Glick, F. X. Haas, A. G. Garrett, P. A. Russo, G. A. Sheppard, M. C. Miller, E. C. Piquette, and T. R. Wenz, "A New Approach to Performing Holdup Measurements on Glove Box Exhausts, *Nucl. Mater. Manage.* **XXI** (Proc. Issue) 64–67 (1991).

8. F. X. Haas, J. B. Glick, J. N. McKamy, A. G. Garrett, P. A. Russo, G. A. Sheppard, T. R. Wenz and M. C. Miller, "Holdup Measurements of Plutonium in Glove Box Exhausts," published in the *Proceedings of the Fifth International Conference on Facility Operation – Safeguards Interface*. LaGrange Park, IL: American Nuclear Society (1991), pp. 237–242.

9. P. A. Russo, M. C. Sumner, T. K. Li, H. O. Menlove, and T. R. Wenz, "Quantitative Verification of In-Process Inventory of High-Burnup Plutonium Using Room-Temperature Gamma-Ray Detectors and the GGH Formalism," Los Alamos National Laboratory report LA-12953-PR (March 1997), pp. 37–48.

10. P. A. Russo, S. E. Smith, and J. F. Harris, "Self-Attenuation and Finite-Source Corrections for Holdup Measurements Automated by the HMS3 Software," Los Alamos National Laboratory document LA-UR-99-4442 (August 1999).

11. S. E. Smith, K. A. Thompson, and R. N. Ceo, "Holdup measurement System 3 (HMS3) User's Guide and Software Documentation," Lockheed-Martin Energy Systems report Y/DK-1104 (1997).

12. S. E. Smith, J. S. Gibson, J. K. Halbig, S. F. Klosterbuer, P. A. Russo, and J. K. Sprinkle, "The Holdup Measurement System II (HMSII)," *Nucl. Mater. Manage.* **XXII** (Proc. Issue) 508-512 (1993).

13. P. A. Russo, J. K. Sprinkle, Jr., J. K. Halbig, S. F. Klosterbuer, and S. E. Smith, "Generalized-Geometry Gamma-Ray Holdup Assay," Los Alamos National Laboratory Application Note LA-LP-94-72 (February 1995).

14. J. L. Parker, "Attenuation Correction Procedures," in *Passive Nondestructive Assay of Nuclear Materials*, D. Reilly, N. Ensslin and H. Smith, Jr, and S. Kreiner, Eds. (NUREG/CR-5550, LA-UR-90-732), Chapter 6, pp.159–194 (March 1991), National Technical Information Service, Springfield, VA.

15. P. A. Russo, J. K. Sprinkle, Jr., C. W. Bjork, T. O. McKown, G. A. Sheppard, S. E. Smith, and J. F. Harris, "Evaluation of the Integrated Holdup Measurement System with the M^3CA for Assay of Uranium and Plutonium Holdup," Los Alamos National Laboratory report LA-13387-MS (August 1999).

16. P. A. Russo, R. Siebelist, J. A. Painter, and J. E. Gilmer, "Evaluation of High-Resolution Gamma-Ray Methods for Determination of Solid Plutonium Holdup in High-Throughput Bulk Processing Equipment," Los Alamos National Laboratory report LA-11729-MS (January 1990).

17. P. A. Russo, T. H Prettyman, S. E. Smith, J. F. Harris, J. S. Massengill, and E. Stair, Jr., "Comparison of Detectors for Portable Gamma-Ray Spectroscopy at Y-12," Los Alamos National Laboratory report LA-UR-99-199 (January 1999).

18. P. A. Russo, A. P. Meier, M. Rawool-Sullivan, T. H. Prettyman, H. Y. Huang, D. A. Close, M. C. Sumner, R. A. Cole, P. N. Luke, and S. A. Soldner, "A New Room-Temperature Gamma-Ray Detector for Improved Assay of Plutonium," *Nucl. Mater. Manage.* **XXVI** (Proc. Issue) CD-ROM (1997).

19. T. H. Prettyman, , M. A. Hoffbauer, M. R. Sweet, P. A. Russo, P. N. Luke, and S. A. Soldner, "Optimization of CdZnTe Detectors for Safeguards," *Nucl. Mater. Manage.* **XXVI** (Proc. Issue) CD-ROM (1997).

20. P. N. Luke. "Single-Polarity Charge Sensing in Ionization Detectors Using Coplanar Electrodes," *Applied Physics Letters*, **65**, No. 22, pp. 2284–2286 (November 28, 1994).

21. P. N. Luke and E. E. Eissler, "Performance of the CdZnTe Coplanar-Grid Detectors," *IEEE Trans. Nucl. Sci.,* **43**, No. 4, pp. 207–213 (August 1995).

22. K. Parnham, "Recent Progress in Cd1-XZnXTe Radiation Detectors," *Nucl. Instr. and Meth. in Physics Research*, **A377**, 487–491 (1996).

23. T. R. Wenz, P. A. Russo, M. C. Miller, H. O. Menlove, T. Takahashi, Y. Yamamoto and I. Aioki, "Portable Gamma-Ray Holdup and Attributes Measurements of High- and Variable-Burnup Plutonium," published in the *Proceedings of the Fifth International Conference on Facility Operation – Safeguards Interface*, LaGrange Park, IL, American Nuclear Society (1991), pp. 226-236.